CHARLES UNIVERSITY IN PRAGUE

FACULTY OF PHARMACY IN HRADEC KRÁLOVÉ

Department of Biochemical Sciences

&

UNIVERSITÉ PARIS DIDEROT – PARIS 7

Laboratoire de Biologie et Biochimie Cellulaire du Vieillissement

OCT ACTIVITY AND GLYCATION DAMAGE IN RAT LIVER MITOCHONDRIA

DIPLOMA THESIS

Supervising: **Dr. Hilaire Bakala**

Prof. MUDr. Jaroslav Dršata, CSc.

Paris, Praha 2007 **Lucie Merhautová**

ACKNOWLEDGEMENTS

My kindest thanks go to Dr. Hilaire Bakala for the possibility to work with him in LBBCV, for his professional leading and reviewing of the manuscript. I gratefully thank Filipe Cabreiro, Martine Perichon, Sylvie Poggioli, Emad Ahmed, Cédric Picot, Anne Laure Bulteau and Caroline Borot for their valuable pieces of advice, technical help and support throughout my stay in the laboratory. I appreciate that the team from laboratory created a pleasant ambience to work in.

My thanks go also to Prof. Dršata for accepting me for this project and advising on the elaboration of this thesis. Finally, I would like to thank all the people around me, who supported me during my stay in the laboratory or writing this thesis.

ABSTRACT

OCT ACTIVITY AND GLYCATION DAMAGE IN RAT LIVER MITOCHONDRIA

This work was created following investigations carried out in LBBCV (Laboratoire de Biologie et Biochimie Cellulaire du Vieillissement) at University Paris Diderot – Paris 7. The team of this laboratory studies the mechanisms of posttranslational non-enzymatic modifications of proteins, involved in the pathophysiology of aging. Glycation is one of the mechanisms responsible for the modification of intracellular macromolecules leading to the loss of their structure and function. In previous investigations, ornithine carbamoyltransferase (OCT), the second enzyme of the urea cycle, has been identified as one of the markedly glycated proteins in liver mitochondria of senescent rats. The goal of this work was to investigate *in vitro* and *ex vivo* glycation of OCT and the effect of glycation on its function. Purified OCT and mitochondrial matrix extracts were incubated with methylglyoxal, one of the most reactive physiological glycating agents, and submitted to the enzymatic assay and immunochemical analysis. We demonstrated that methylglyoxal modifies OCT both *in vitro* and *ex vivo* and causes rapid and extensive decrease in its enzymatic activity. According to this study, carboxyethyllysine and cross-linked AGEs are formed. We also confirmed that MGO exerts a negative effect on mitochondrial respiration.

ABSTRAKT

AKTIVITA OCT A GLYKAČNÍ POŠKOZENÍ V MITOCHONDRIÍCH JATER KRYSY

Tato práce byla vytvořena na základě pokusů provedených v LBBCV (Laboratoři buněčné biologie a biochemie stárnutí) v rámci Univerzity Paris Diderot – Paris 7. Tým této laboratoře studuje mechanismy posttranslačních neenzymatických modifikací proteinů, zahrnutých v patofyziologii stárnutí. Glykace je jedním z mechanismů odpovědných za modifikaci nitrobuněčných makromolekul, které vedou ke ztrátě jejich struktury a funkce. Ornitin karbamoyltransferáza (OCT), druhý enzym močovinového cyklu, byl v předchozím výzkumu identifikován jako jeden z enzymů, které jsou významně glykovány uvnitř mitochondrií jater stárnoucích krys. Cílem této práce bylo sledovat glykaci OCT *in vitro* a *ex vivo* a její vliv na funkci tohoto enzymu. Vzorky purifikované OCT a extraktů mitochondriální matrix byly inkubovány s methylglyoxalem, jedním z nejreaktivnějších fyziologických glykačních činidel. U vzorků byla změřena enzymatická aktivita a byly podrobeny imunochemické analýze. Podařilo se nám prokázat, že methylglyoxal modifikuje OCT jak *in vitro*, tak *ex vivo*, a způsobuje velice rychlý a rozsáhlý pokles jeho enzymatické aktivity. Podle výsledků této studie vznikají karboxyethyllysinové zbytky a tzv. zřetězené pozdní glykační produkty (cross-linked AGEs). Potvrdili jsme také negativní vliv methylglyoxalu na mitochondriální dýchání.

TABLE OF CONTENTS

1 INTRODUCTION

This work was created following investigations carried out in Laboratoire de Biologie et Biochimie Cellulaire du Vieillissement (LBBCV) at University Paris Diderot – Paris 7. The team of this laboratory studies the mechanisms of posttranslational non-enzymatic modifications of proteins, involved in the processes of pathophysiology of aging.

Aging, an inevitable biological process, is characterized by the gradual decline in celluar functions. Glycation is one of the mechanisms responsible for the modification of intracellular macromolecules leading to the loss of their structure and function. The accumulation of damaged molecules can contribute to the general decline observed in this process. Mitochondria, the main sites of energy production within the living cell, are believed to have the key role in cellular aging. The team of LBBCV demonstrated, that only a restricted set of proteins is modified by glycation during aging in rat liver mitochondria. Ornithine carbamoyltransferase (OCT), the second enzyme of the urea cycle, has been identified as a target of glycation damage. This work is focused on the study of the effects of glycative modifications on the activity of OCT.

2 GENERAL PART

2.1 AGING AND GLYCATIVE DAMAGES

Aging, an inevitable biological process, is characterized by a general decline in physiological function that leads to morbidity and mortality. It is believed that the age-related deficits in mitochondrial function, especially the decline in ATP production, are the main contributors to the process of cellular aging and the generalized physiological decline [1]. Aging is associated with an increase in reactive oxygen species (ROS) production and an accumulation of macromolecules damaged by post-translational non-ezymatic modifications which alter the structure and function of tissue and cellular macromolecules, especially proteins. Under oxidative stress, carbohydrates, lipids and proteins are the major targets of ROS. Proteins can be damaged either directly (oxidative damage) or indirectly through the reactive carbonyl compounds derived from the oxidation of carbohydrates (glycoxidative damage) and lipids (by products of lipid peroxidation) [2].

Glycation (non-enzymatic glycosylation) is another type of protein modification associated with aging and is accelerated in diabetes. The reactions of reducing sugars with amino groups of peptides and proteins, resulting in the formation of complex brown pigments and protein-protein crosslinks, were for the first time described by food chemists Maillard and Gautier in the early 1900s. Later on, this type of reactions, referred to as Maillard reactions, was observed *in vivo*. Its later-stage products, called advanced glycation end-products or AGEs, were proposed around 1980 to be linked with diabetic complications and aging. A large body of evidence has been accumulated implicating AGEs as mediators of these processes [3].

AGEs can be formed from reactive intermediates of Maillard reaction (i.e. glucose and other reducing sugars), but also from reactive dicarbonyl compounds (such as glyoxal, methylglyoxal, 3-deoxyglucosone) derived from glycolytic triose phosphate intermediates, metabolites of the polyol pathway or other metabolic pathways. Since most of the AGE-related reactions comprise oxidation and AGE formation is enhanced by oxidative stress and reversely, the processes of glycation, glycoxidation and lipoxidation are closely connected and these terms are often replaced [4].

2.1.1 The „Classical“ Glycation Pathway

Protein glycation is initiated by a nucleophilic addition reaction between a carbonyl group from a reducing sugar (e.g. glucose, fructose, ribose) and a free amino group of protein (mainly on Lys and Arg residues). This reaction, occurring over a period of hours, is highly reversible and therefore reactant-concentration dependent. The resulting Schiff base (aldimine intermediate) is unstable and undergoes a chemical rearrangement (called Amadori rearrangement) to form a more stable ketoamine linkage (Amadori product) (Figure 1). The formation of the Amadori product is slower (over a period of days), but practically irreversible. The Amadori product thus tends to accumulate on proteins [3].

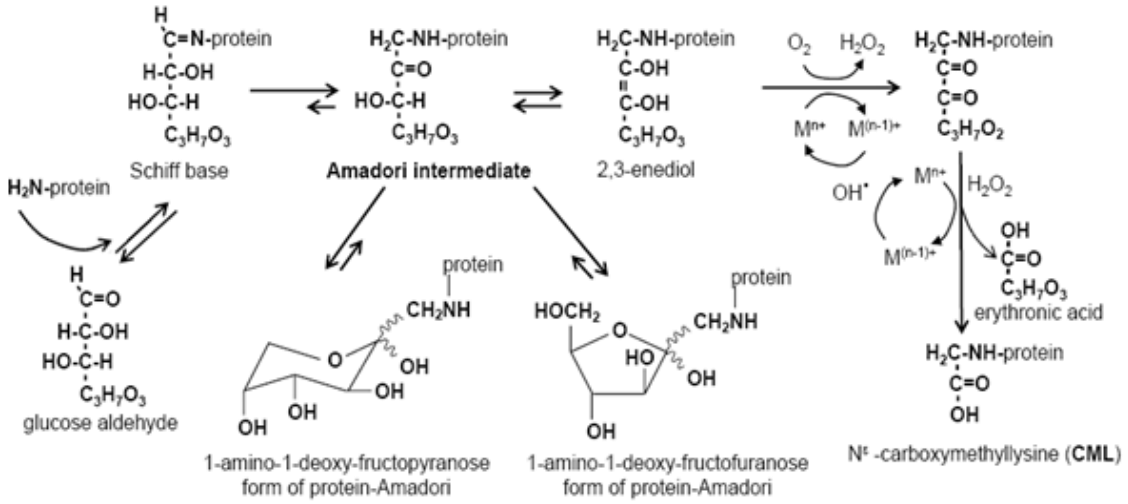

Figure 1. Pathway of formation of glucose-derived protein-Amadori product and protein-CML [5]

A less-well-understood process of advanced glycation begins subsequently to the Amadori rearrangement. A glycated protein can undergo further non-enzymatic modification through dehydration, cyclisation, fragmentation or rearrangement reactions. These reactions occur under both oxidative and non-oxidative conditions and give rise to imperfectly characterised structures called advanced glycation end-products (AGEs) [3].

Ambient concentration of glucose (and glycating agents in general), duration of protein exposure, its structure and turnover half-life are important determinants of the glycation rate. The amount of a glycated protein *in vivo* is reflected by a balance between its formation and degradation [6].

2.1.2 Alternative Glycation Pathways

Recent studies have provided convincing evidence that glycation of proteins may be initiated by various mechanisms and pathways not solely or necessarily by the Amadori degradation process. In this context, the Schiff base has been recognized as a source of dicarbonyl compounds and ROS undergoing the Namiki pathway. Alternative pathways for generation of glycated proteins shown in Figure 2 include glucose auto-oxidation, the polyol pathway, triose phosphate fragmentation and catabolism of ketone bodies generating methylglyoxal, and lipid peroxidation products such as malondialdehyde and 4-hydroxy-2-nonenal (HNE) [6].

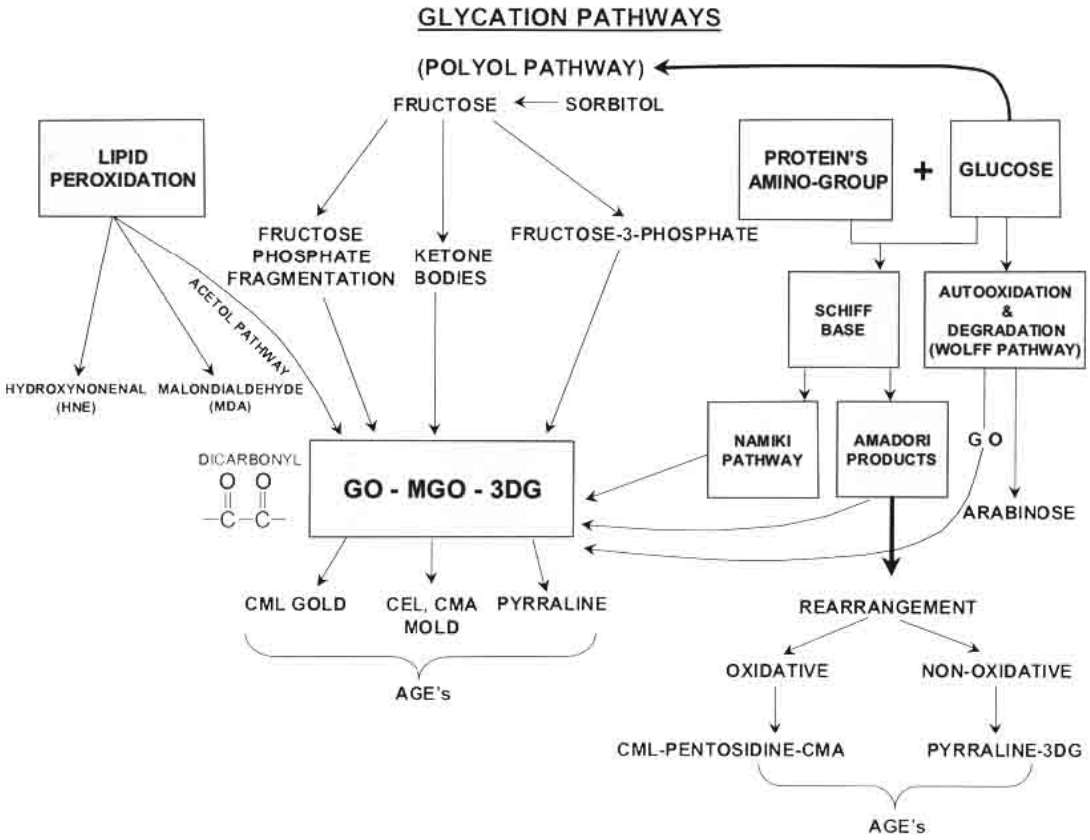

Figure 2. Glycation pathways [6]

An important step in the glycation reactions is the generation of reactive intermediate products in the course of all stages and pathways of glycation. These compounds are known as α-dicarbonyls, and include such products as 3-deoxyglucosone (3-DG), glyoxal (GO) and methylgoxal (MGO). 3-DG is formed by non-oxidative rearrangement and hydrolysis of the Amadori product and by fructose-3-phosphate, an intermediate of the polyol pathway. MGO is produced from

oxidative and non-oxidative reactions in several pathways shown in Figure 2, but also as a by-product of triosephosphate metabolism in glycolysis [6, 7]. Glyoxal is formed from several reactions such as oxidative fragmentation of the Schiff base (Namiki pathway), lipid peroxidation (Acetol pathway), and fructose-phosphate fragmentation. 3-DG inactivates glutathione peroxidase, an enzyme responsible for the detoxification of hydrogen peroxide, which leads to increased cellular oxidative stress. It also inactivates glutathion reductase, an antioxidative enzyme. However, major inactivation of glutathione reductase is caused by HNE. The accumulation of MGO and other reactive dicarbonyl compounds, from both glycoxidation and lipoxidation sources (due to ROS overproduction), is called carbonyl stress [6].

It is noteworthy that glucose is the least reactive of the common sugars, perhaps leading to its evolutionary selection as the principal free sugar in vivo. It has become increasingly clear that highly reactive α-dicarbonyl compounds are the key intermediates in the formation of AGEs [3].

2.1.3 Methylglyoxal

Methylglyoxal (MGO, pyruvaldehyde, 2-oxopropanal), a physiological but chemically highly reactive α-dicarbonyl metabolite of glucose degradation pathways, is thought to be the major source of intracellular and plasma AGEs in diabetes [8].

During glucose metabolism triose phosphates may undergo either spontaneous or enzyme-facilitated decomposition to yield MGO. The active site of triose phosphate isomerase harbours a flexible loop surrounding enzyme-bound reaction intermediate. This loop flickers continuously between open and closed states leading to a small but constant leakage of unstable intermediate enediolate phosphate that immediately undergoes phosphate elimination to yield MGO. Triose phosphate isomerase is present at high concentration in tissues, and therefore significant amounts of MGO and MGO-modified proteins may be produced [9].

Methylglyoxal is also formed from acetone by cytochrome P450 2El which catalyses the sequential formation of hydroxyacetone and methylglyoxal, by methylglyoxal synthase and by the oxidation of aminoacetone formed in the catabolism of threonine. The major source of methylglyoxal formation in human red blood cells in vitro under normoglycaemic conditions was the non-enzymatic fragmentation of triosephosphates [7].

At physiological concentrations MGO primarily targets the arginine residues of proteins, resulting initially in the formation of reversible adducts. These adducts may consequently undergo a series of rearrangements that yield several possible end-products that contain either imidazolone- or pyrimidine-based ring systems [9]. MGO is also highly reactive with lysine, sulfhydryl groups on proteins and nucleic acids, inducing the formation of a variety of structurally identified AGEs (Figure 3) [8].

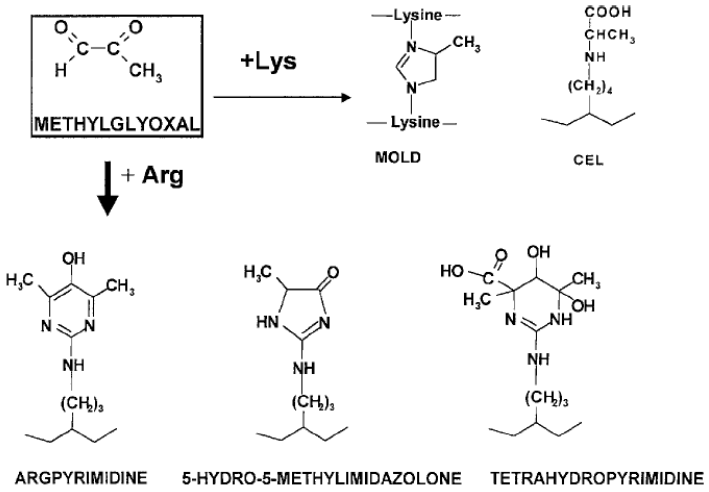

Figure 3. Methylglyoxal-derived AGEs [10]

The formation of MGO occurs in all cells and organisms and it represents about 0,1% of the flux of glucotriose under normoglycaemic conditions. Such a small fraction of glucotriose flux is, however, important because of the high reactivity of methylglyoxal. If methyglyoxal was not efficiently detoxified, it would induce mutagenicity and protein degradation. MGO is detoxified by conversion to lactate catalyzed in the cytosol of all cells by the glyoxalase system. Glyoxalase system comprises glyoxalase I, catalyzing the formation of S-D-lactoylglutathione, and glyoxalase II, converting the S-D-lactoylglutathione into D-lactate. Methylglyoxal can be also metabolized by aldose reductase, an NADPH-dependent aldehyde reductase involved in the detoxification of aldehydes and osmoregulation. MGO is converted to hydroxyacetone (95%) and o-lactaldehyde (5%) [7].

The determination of MGO concentration in living cells is complicated, since > 90 % of MGO is reversibly bound to cellular protein. Physiologic concentrations of free MGO are considered as < 5 μM [7], while the concentration of total intracellular MGO has been reported to be as high as 310 μM in cultured Chinese hamster ovary

cells [11]. The formation of MGO is increased in hyperglycaemia associated with diabetes mellitus [7] and involved in the pathophysiology of aging [12].

2.1.4 Advanced Glycation End-products

AGEs are heterogeneous compounds derived from glucose and other reactive carbonyls interacting with biological macromolecules. Many of these cross-linking or non-cross-linking compounds are chromophores or fluorophores [3]. More than a dozen AGEs have been detected in tissue proteins (Figure 4) [4].

They can be divided as follows [13]:

A. Fluorescent cross-linking AGEs: pentosidine, crosslines, vesperlysines, fluorolink. Pentosidine is an Arg-Lys cross-link, glycoxidative product formed by a reaction with any of the carbohydrate precursors (3-DG, glucose, ribose, ascorbic acid).

B. Non-fluorescent cross-linking AGEs: imidazolium dilysine cross-links: glyoxal-derived lysine dimer (GOLD) and methylglyoxal-derived lysine dimer (MOLD); arginine-lysine cross-links: glyoxal-derived imidazoline cross-link (GODIC) and methylglyoxal-derived imidazoline cross-link (MODIC); glucosepan, 1-alkyl-2-formyl-3,4-diglucosyl-pyrrole (AFGP), arginine-lysine imidazole (ALI) etc. GOLD, MOLD, GODIC, MODIC and glucosepane have been shown to be the major *in vivo* cross-links [14]. A recent work indicated that glucosepane is the major cross-link in extracellular matrix of senescent rats [15].

C. Non-cross-linking AGEs: pyrraline, carboxymethyllysine (CML), carboxyethyllysine (CEL), carboxymethylarginine (CMA), imidazolones, hydroimidazolones, argpyrimidine.

CML, CEL, GOLD, MOLD, GODIC, MODIC, CMA, hydroimidazolones and argpyrimidine can be formed both by glycoxidation and lipoxidation pathways, and therefore are also referred to as advanced lipoxidation end-products (ALEs) [16].

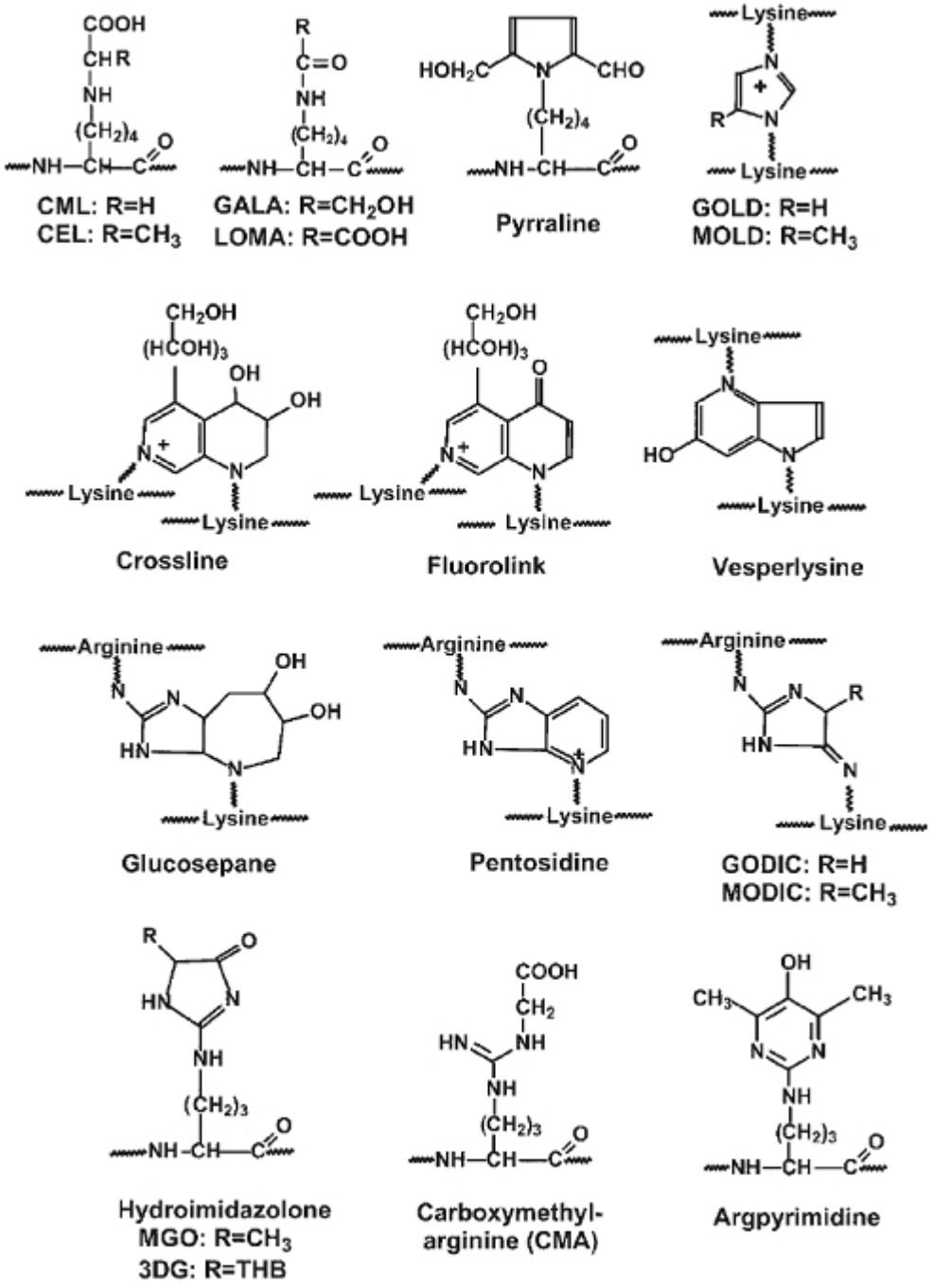

Figure 4. Structures of AGEs that have been detected in tissue proteins [16]

The accumulation of blood or tissue AGEs is characteristic not only of diabetes and the normal aging process, but is also associated with atherosclerosis and most, if not all, age-related, chronic diseases, including rheumatoid arthritis, amyloidosis, Alzheimer's and other neurodegenerative diseases [4]. AGE formation causes pathological changes via three general mechanisms. First, AGEs alter several important matrix components, such as collagen, and impair normal vascular function. Second,

AGEs trigger the inflammatory response through interactions with AGE-specific cellular receptors. Third, intracellular AGE formation can directly alter protein function in target tissues [17].

Although AGEs were initially thought to arise only on long-lived extracellular proteins (such as collagen or crystalline) [4], recent quantitative study in diabetics has shown even higher levels of intracellular AGEs compared to plasma proteins [18]. The impact of AGE formation on short-lived proteins (including circulating plasma proteins and cytoplasmic proteins) is attenuated by their high turnover. Nevertheless, such modification is associated with accelerated oxidative damage, reduced degradative capacity, disruption of molecular conformation, decreased ligand binding, modified immunogenicity and altered enzymatic activity [19].

However, little is known about intracellular and even less about subcellular targets of glycation-induced damage. Intracellular AGE formation is a ROS-dependent process [20]. Besides the structure (number and accessibility of reactive residues), the protein's susceptibility to glycation is influenced by the type of glycating agent, the presence of substrates or cofactors (in the case of an enzyme) and the presence of protecting compounds (e.g. carnosine, chaperones, glycating agent metabolising enzyme) [21].

Only a restricted set of proteins is affected by glycoxidative modification in cytosol of aged human lymphocytes [22]. Within 7 days, a 14-fold increase in the amount of total intracellular AGEs occurred in endothelial cells cultured under high glucose conditions, compared with controls. The basic fibroblast growth factor (bFGF) has been found as one of the main AGEs-modified proteins and its alteration has been proved to be responsible for a markedly decreased heparin binding capacity and mitogenic activity [23]. The function of heat shock protein 27 (Hsp27), the major target of glycation in glomerular mesangial cells cultured in a high-glucose medium, was also altered [24].

There is evidence that these enzymes are inhibited by glycation: glucokinase, 2-oxoglutarate dehydrogenase, alanine aminotransferase, aspartate aminotransferase, lactate dehydrogenase, glyceraldehyde-3P dehydrogenase, creatine kinase, Na+/K+ATPase, DNA polymerase, ribonuclease A, alkaline phosphatase, acylphosphatase, glutathione reductase, glutathione peroxidase, glucose-6P dehydrogenase, glutathione S-transferase, aldehyde reductase, glyoxalase, sorbitol dehydrogenase, catalase, superoxide dismutase, alcohol dehydrogenase,

Spot No.	Protein UniProt Accession No.	Mass kDa	pI	Peptides matches	Coverage (%)

bisphosphoglyerate mutase, porphobilinogen deaminase, carbonic anhydrase and others [21]. Naturally, glycation of an enzyme need not result in its inhibition [25].

Mitochondrial proteins may be the target of glycation reactions, as well as those from cytosol. Recently, the MGO-induced inhibition of mitochondrial respiration has been explored [8], increased levels of AGEs have been found in the mitochondrial proteins of aged [2] and diabetic rats [26] and several target proteins have been identified. Rosca et al. identified 7 proteins modified by MGO, which belonged to two pathways: oxidative phosphorylation and ß-oxidation. Two of these proteins were components of respiratory *complex III*, the major site of superoxide production in health and disease. The activity of this complex was significantly decreased in diabetic rats, in correlation with increased superoxide formation and increased quantity of MGO-modified proteins present in mitochondria. Interestingly, the functions of MGO-modified *complex I*, ATPase and components of ß-oxidation pathway seem to be unchanged [26].

Bakala et al identified three significantly AGE-modified proteins in liver mitochondria of aged rats (unpublished work). 2D Western blot analysis with anti-AGE antibody (Figure 5) followed by tandem mass spectrometry helped to identify glutamate dehydrogenase (GDH), catalase and ornithine carbamoyltransferase (OCT) (Table 1 and Figure 6). Incubation of GDH with MGO resulted in loss of enzymatic activity in a dose- and time-dependent manner [27]. These results led to the present work: to investigate whether MGO has an influence on enzymatic activity of OCT.

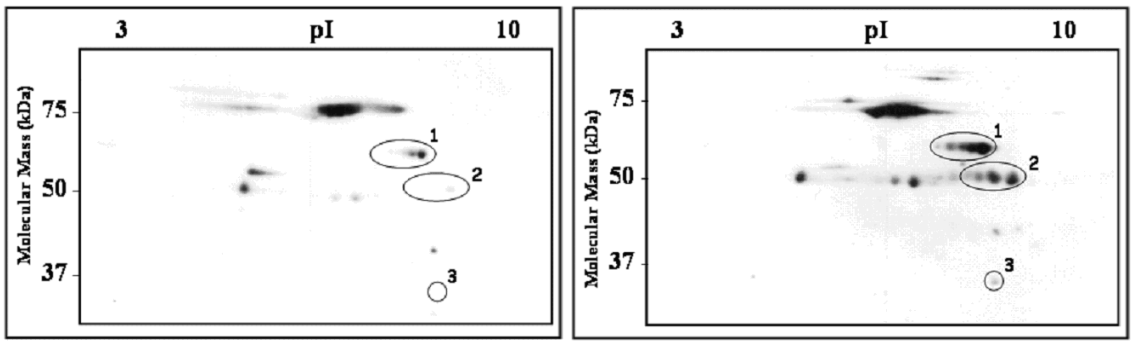

Figure 5. 2D Western blot analysis with anti-AGE antibody - young and aged rat. Extracts of mitochondrial proteins from liver of young (left panel) and aged (right panel) rats were separated by 2D electrophoresis and subjected to Western blot analysis with anti-AGE antibody. Three spots, significantly more labelled in aged animals, were excised from identical gels and identified by means of tandem mass spectrometry technique. 1 – GDH, 2 – catalase, 3 – OCT

3	Ornithine carbamoyltransferase, mitochondrial, P00481	39.9	9.12	10		32	

Sequence	Position	MH^+	ΔM	z	Xc
K.GRDLLTLK.N	39-46	915.56	0.51	2	2.17
K.GEYLPLLQGK.S	71-80	1117.63	0.36	2	2.42
R.VLSSM*TDAVLAR.V	130-141	1278.67	0.57	2	3.41
R.VYKQSDLDILAK.E	142-153	1392.77	0.53	2	2.01
K.FGM*HLQAATPK.G	211-221	1216.61	0.43	2	2.20
K.GYEPDPNIVK.L	222-231	1131.57	0.26	2	2.07
K.LSM*TNDPLEAAR.G	244-255	1333.64	0.20	2	3.23
R.LQAFQGYQVTM*K.T	278-289	1429.71	0.54	2	3.98
R.KPEEVDDEVFYSPR.S	307-320	1709.80	0.71	2	2.91
R.SLVFPEAENR.L	321-330	1161.60	0.62	2	2.87

Table 1. Peptides from OCT identified by tandem mass spectrometry technique

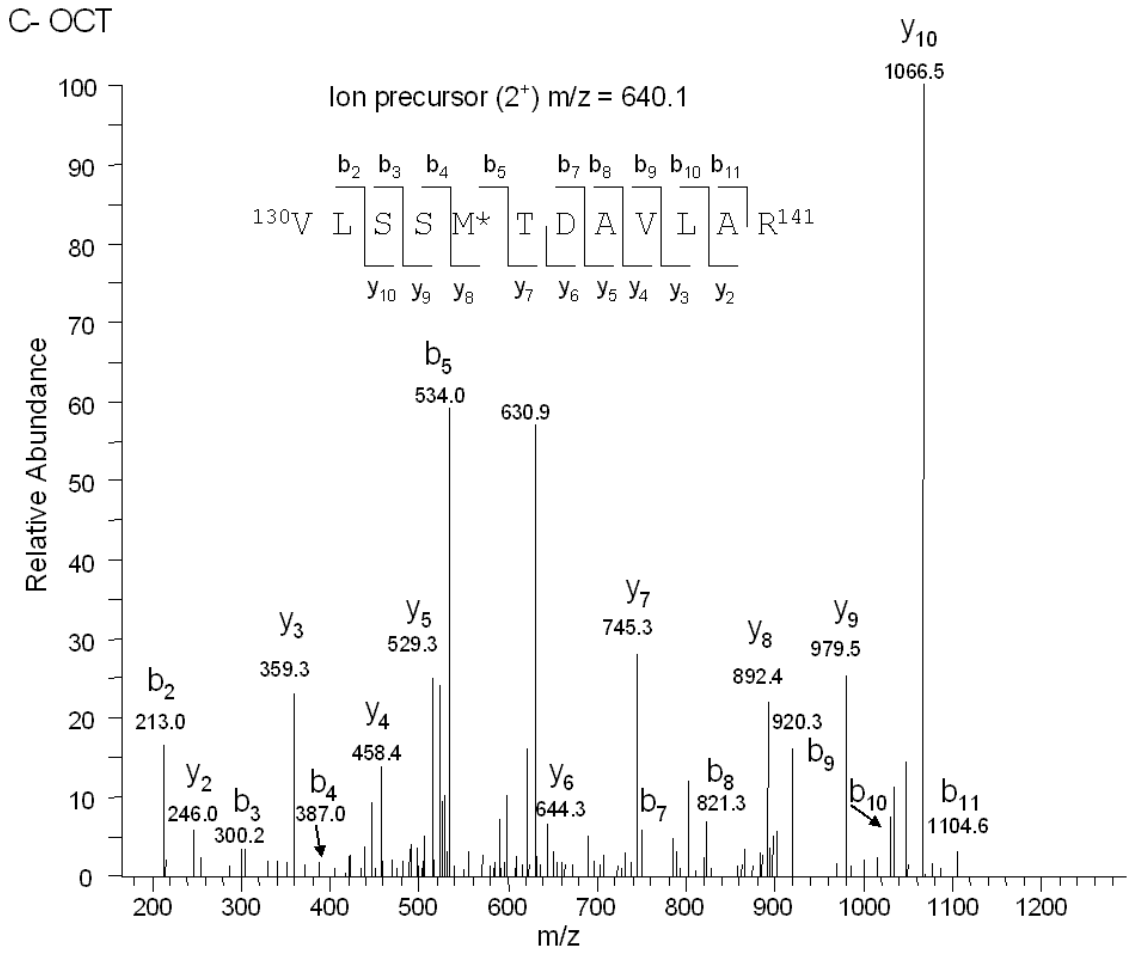

Figure 6. Example of MS/MS spectre of one peptide from OCT – peptide m/z = 640,1; charge = 2

2.2 ORNITHINE CARBAMOYLTRANSFERASE

Ornithine carbamoyltransferase (OCT, EC 2.1.3.3), also referred to as ornithine transcarbam(o)ylase (OTC, OTCase), catalyzes the conversion of ornithine and carbamoylphospahe into citrulline and phosphate (Figure 7) in the urea cycle or in the biosynthesis of arginine (anabolic OCT) [28]. In some microorganisms, an OCT catalyzes the reverse reaction in the deiminase pathway for arginine degradation (catabolic OCT) [29].

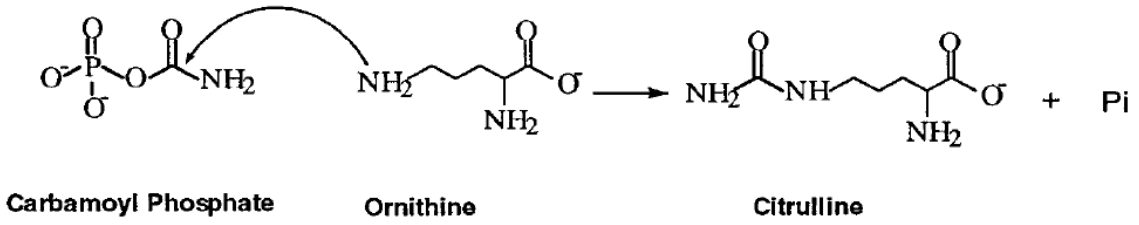

Figure 7. Reaction catalyzed by OCT [30]

Anabolic OCTs usually occur as trimeric molecules with subunits of 35-40 kDa in molecular mass, but the anabolic OCT from *Pyrococcus furiosus*, a thermophilic archaebacterium is a dodecamer [28]. OCT from *Streptococcus faecalis* seems to be a hexamer [31]. Catabolic OCTs are usually larger than anabolic OCTs with 12 identical subunits in the holoenzyme and display pronounced allosteric behaviour [28].

2.2.1 Structure of Human, Rat and *Streptococcus faecalis* OCT

Recently, detailed structure and catalytic mechanism of the human ornithine carbamoyltransferase were studied by Shi et al. [28, 30, 32]. Rat and *Streptococcus faecalis* (i.e. *Enterococcus faecalis*) OCTs were used for our experiments, so it was useful to compare the structures of these 3 enzymes. The sequences were aligned and compared by CLUSTALW (Figure 8). Only 30 % of residues were identical, 20 % were considered strongly similar and 10 % weakly similar. Rat and human OCTs, when compared together, had 92 % identical and 4 % strongly similar residues.

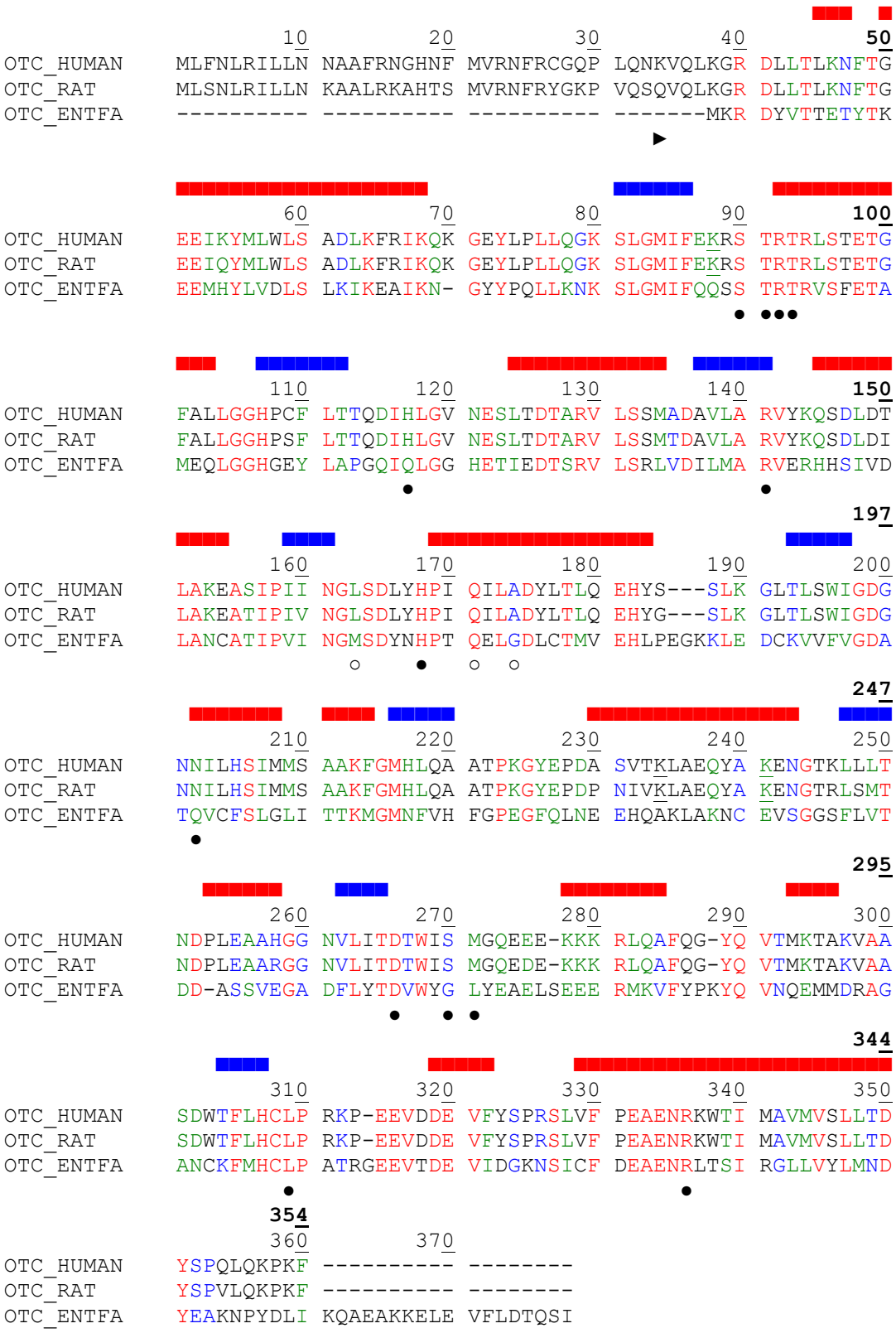

Figure 8. Sequence alignment of human, rat and *Streptococcus faecalis* OCT (precursors). ■ α-helix, ■ β-strand, ● residues involved in PALO binding, ○ residues proposed to be involved in the catalytic mechanism, K N_6-acetyllysine, red residues are identical (30 %), green residues strongly similar (20 %), blue residues weakly similar (10 %) and black residues different (40 %), numbers in **bold** correspond to the human sequence, ► human and rat OCT chain starts. Sequence data is retrieved from the UnitProt Knowledgebase [33] and aligned by CLUSTALW [34]. Secondary structure and catalytic mechanism are adopted from Shi et al. [32]

Interestingly, comparing the 3D-structure of subunits of these 3 enzymes (Figure 9), there are no striking differences. This fact supports the theory of a common gene ancestor for all 44 OCTs whose sequences are known to date [35]. For these reasons, we can consider purified OCT from *Streptococcus faecalis* a useful model for our experiments with rat liver extracts.

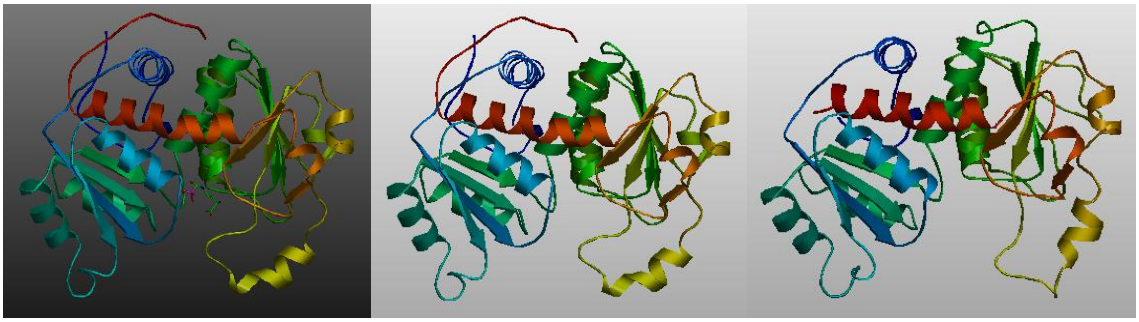

Figure 9. 3D-structure of human, rat and *Streptococcus faecalis* OCT (from left to right). N-terminus is coloured *blue*, C-terminus *red*. Bisubstrate analog PALO is added to the human OCT model. The model of *S. faecalis* OCT is created from residues 3 to 309 (of total 339). Images are created by AstexViewer2.0 [36], which displays the protein structures at SWISS-MODEL Respository website [37].

Human ornithine carbamoyltransferase consists of three identical subunits (Figure 10). Each subunit is composed of two domains: a CP binding domain (residues 34-168 and 345-354) and ornithine binding domain (residues 183-322). The extended C-terminus (residues 345-354) found only in mammalian OCTs, is part of the CP domain. The structure of OCT comprises 14 α-helices and 9 β-sheets. In the Figure 9, the CP domain is coloured from blue to bluish-green plus red C-terminus (the left part of the molecule), the ornithine domain is coloured from green to yellow and orange (the right part of the molecule). Since the loop between residues 263 and 286 contains a conserved Ser-Met-Gly sequence, it is referred to as the SMG loop [32] (the yellow loop in the Figure 9). According to Shi et al. [32], the SMG motif is present in all 33 known OTC sequences, but in OCT from *Streptococcus faecalis*, it is not found. This fact could be explained by Naumoff et al. [38]. His team has recently shown that the gene argF-2 (according to UniProt Knowledgebase encoding OCT) encodes another type of carbamoyltransferase: putrescine carbamoyltransferase (PTCase, EC 2.1.3.6). These two enzymes could be confused because of their high sequence similarity.

The active site is located in the cleft between the domains. In the catalytically active trimer, the CP binding domains are located in the interior of the protein and the binding domains for the second ligand are external. The interface between the subunits is formed primarily by residues from the CP domains [32].

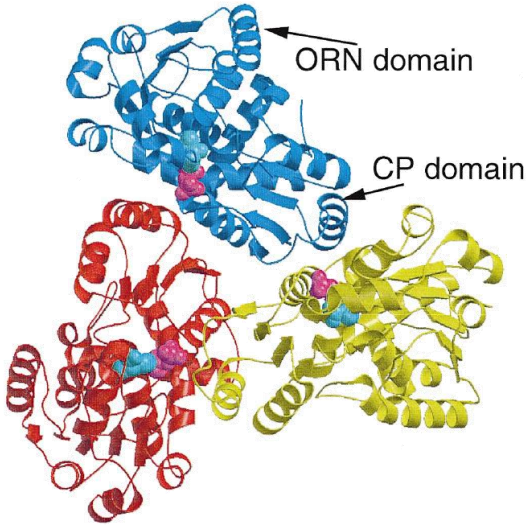

Figure 10. Ribbon diagram of the human OCT catalytic trimer. The three subunits are coloured *blue*, *red* and *yellow*, the CP and ORN are shown as a space filling model coloured *pink* and *light blue* respectively [30].

The structure of the active site with the bisubstrate analog N-phosphonacetyl-L-ornithine (PALO) is shown in Figure 11. Residues involved in PALO binding are indicated by a filled circle in Figure 8. His-117 binding to one of the phosphonate oxygen of PALO is from an adjacent subunit in the catalytic trimer [32]. There are three Arg and one Lys susceptible of modification by methylglyoxal in the active site. The possibility of Cys modification by methylglyoxal should be also considered.

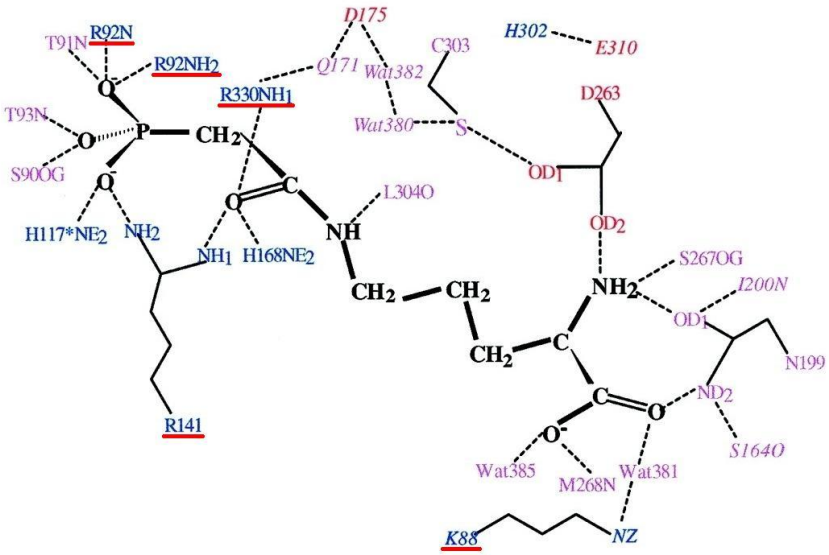

Figure 11. Schematic view showing the interaction of the bisubstrate analog PALO with human OTCase active site residues. PALO is showed in *bold*. The residue indicated with * is from adjacent subunit. Wat = water molecule [32]. *Red underlining* highlights Arg (R) or Lys (K) residues, which can be theoretically modified by methylglyoxal.

The conserved STRTR motif in OCTs, long recognized as the site for CP binding, is involved in binding the phospate group. HPXQ involved in binding the carbamoyl group of CP is the second conserved motif. HCLP motif is part of the ornithine binding site. It probably stabilizes the tetrahedral intermediate, rather than being essential for binding the second substrate [28]. This motif is present also in PTCases and binds the substrate putrescine [38]. The conserved DXXXSMG motif from the flexible SMG loop is the main binding site for L-ornithine in OCT [28]. The lack of this motif in the putative *S. faecalis* OCT sequence from UniProt Knowledgebase supports Naumoff's theory [38].

The C-terminal extension of human OCT is proposed to be involved in mediating interactions with the membrane, because it is exposed on the convex face of the enzyme and contains a sequence motif characteristic of membrane-associated proteins. Indeed, electron microscopy indicates that OCT is associated with the mitochondrial membrane [32].

Molecular mass, number of total amino acid residues and number of Lys and Arg residues of human, rat and *S. faecalis* OCT are compared in Table 2. Mammalian precursors contain the targeting sequence, which enables the enzyme to be imported into the mitochondrion and which is removed after import [39].

	Precursor	Enzyme	Lys Arg
Human	39,9 kDa 354 aa	36,1 kDa 322 aa	26 (8,1 %) 11 (3,4 %)
Rat	39,9 kDa 354 aa	36,2 kDa 322 aa	23 (7,1 %) 13 (4 %)
S. faecalis		38,3 kDa 339 aa	21 (6,2 %) 12 (3,5 %)

Table 2. Comparison of human, rat and *S. faecalis* OCT. Data from UniProt Knowledgebase and its ProtParam tool [33]

2.2.2 Catalytic mechanism of OCT

Cys-303 appears to play a central role in the catalytic mechanism of human OCT (Figure 12). The side chain of Cys-303 forms a hydrogen bond with Asp-263, which is expected to stabilize the thiolate form of the sulfhydryl group, enabling it to accept a proton from the δ-amino group of ornithine and thus facilitating nucleophilic attack on the carbonyl carbon of CP. The tetrahedral intermediate can be stabilized both by Gln-171, which is positioned so as to be able to form a hydrogen bond to the positive

N-δ of ornithine, and by Arg-141, Arg-330 and His-168, which form hydrogen bonds to the negative carbonyl oxygen of CP [32].

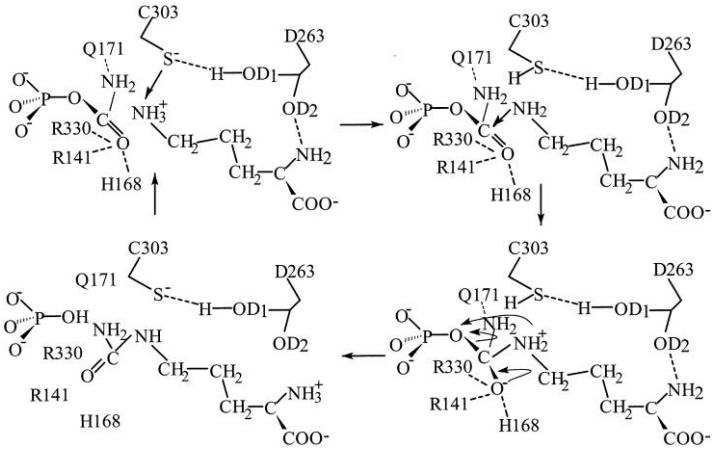

Figure 12. Schematic drawing of a possible catalytic mechanism [32]

The recent study of Shi et al. [28] has revealed that the binding of the first substrate, CP at the base of the catalytic cleft, induces a global conformational change involving relative domain closure, whereas the binding of the second substrate brings the flexible SMG loop into the active site to cover the catalytic cleft.

2.2.3 The Role of OCT and the Urea Cycle

Human ornithine carbamoyltransferase, catalyzing the second reaction of the urea cycle, is expressed in the liver and gut [40]. The liver is generally thought to be the only organ with a complete urea cycle [41], representing the sole mechanism for ammonia disposal in man [42]. Since ammonia is a toxic compound, this enzyme is essential for human life [41, 32].

The urea cycle, for the first time described by Hans Krebs and Kurt Henseleit in 1932, comprises 5 enzymatic reactions (Figure 13). The first two steps take place in mitochondria, while the rest of the cycle is performed in the cytosol. Firstly, carbamoyl phosphate synthetase I catalyses the formation of CP from HCO_3^- and NH_4^+ (while CPS II is involved in pyrimidine biosynthesis). CP is then transferred by OCT to ornithine, to form citrulline. Citrulline is afterwards conjugated with aspartate by argininosuccinate synthetase and resultant argininosuccinate is cleaved into arginine and fumarate by arginosuccinate lyase. Finally, arginase releases urea and ornithine, which is subsequently ready to accept another CP molecule. Urea, created from

hydrogencarbonate carbon, one nitrogen from ammonia and the second one from aspartate, is a relatively non-toxic excretion product that is eliminated by the kidneys [43].

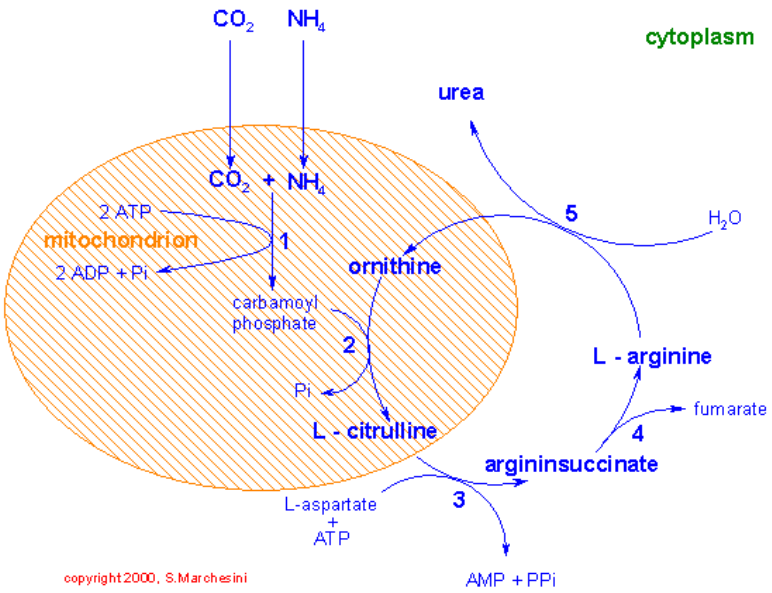

Figure 13. The urea cycle. 1 – Carbamoyl phosphate synthetase I, 2 – Ornithine carbamoyltransferase, 3 – Argininosuccinate synthetase, 4 – Argininosuccinate lyase, 5 – Arginase

The urea cycle is closely linked to the tricarboxylic acid cycle (TCA cycle, citric acid or Krebs cycle) (Figure 14). These two metabolic cycles are connected by the formation and degradation of argininosuccinate. Oxaloacetate from TCA cycle gives rise through transamination to asparate, the donor of the second nitrogen forming urea. Fumarate released by the argininosuccinate cleavage returns back to the TCA cycle to regenerate oxaloacetate [43].

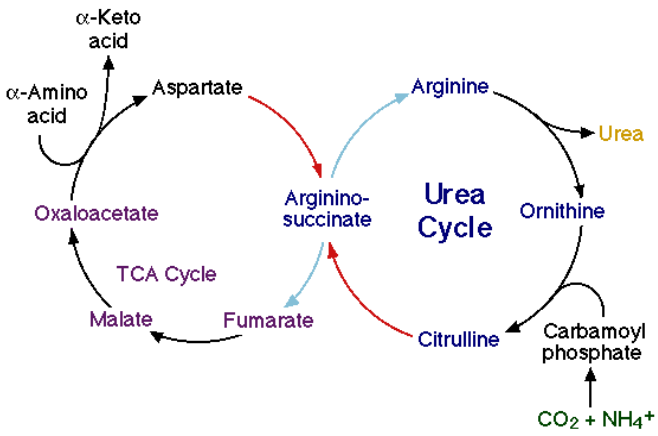

Figure 14. TCA and urea cycles are connected by formation and degradation of argininosuccinate [44]

There is another important connection between urea and TCA cycle. Because the most of amino acids are degraded through transamination, where the prepondering acceptor of the amino group is α-ketoglutarate (TCA cycle substrate), the main product of amino acid catabolism is glutamate. Glutamate can be then oxidatively deaminated by glutamate dehydrogenase (GDH) to form ammonia or transaminated to form aspartate. In both cases, α-ketoglutarate is regenerated. Resulting ammonia and aspartate enter the urea cycle to form urea. Ornithine, the acceptor of CP in the urea cycle, is also derived from glutamate. Hence, there is no surprise that the urea cycle is regulated by glutamate concentration: glutamate is a substrate for N-acetylglutamate formation, an obligatory activator of CPS I, the first step of the urea cycle. The rest of the cycle is regulated by concentration of substrates [43, 41].

The urea cycle consumes 3 ATP molecules, which are hydrolyzed to 2 ADP and one AMP. These energetic requirements are more than compensated by the energy released with the formation of urea cycle substrates: NAD(P)H produced by oxidative deamination of glutamate and NADH formed by transformation of fumarate into oxalacetate in TCA cycle [43].

Glutamine has an important role in nitrogen metabolism. It is quantitatively the most significant nitrogen transporter between tissues and its synthesis serves as a detoxification of excess ammonia in extrahepatic tissues [45]. Glutamine is the most abundant amino acid in the body and in some cells (e.g. thymocytes, macrophages and lymphocytes) serves as the major respiratory substrate. Its circulating levels are regulated by the liver, using glutamine as a substrate for urea synthesis and gluconeogenesis (Figure 15) [46].

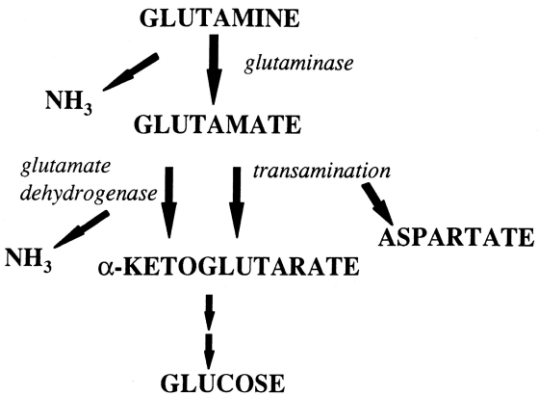

Figure 15. Glutamine catabolic pathways [45]

Interestingly, hepatic glutaminase is activated by its own product, ammonia. Although positive feedback seems to be bizarre in the metabolic control system, in this place it is very effective. Activation of glutaminase provides glutamate to form N-acetylglutamate, which unleashes the whole urea cycle and the excess ammonia (and glutamine) can be eliminated from the body [41].

OCT is also present in small intestine enterocytes, which have an important role in the endogenous synthesis of arginine in most mammals [47]. Although all urea cycle enzymes are present to some extent in the small intestine and Wu demonstrated urea synthesis in entrecotes from weaned pigs, it is nonetheless clear that the major product of these enzymes in the small intestine is citrulline, not urea [48].

2.2.4 Ornithine CarbamoylTransferase Deficiency

Ornithine carbamoyltransferase deficiency (OCTD, also OTCD in literature), the most common urea cycle defect, is heterogeneous in its presentation. OCTD can be divided into two groups: neonatal onset type and late onset type. Neonatal OCTD is mainly presented in males, since the gene encoding OCT is located on Xp21.1. This type is connected with abolished enzyme activity and it is likely to be lethal, if untreated. Late onset OCTD, mainly presented in female heterozygotes, show partial and varying enzyme deficiency. In this type, symptoms usually occur together with precipitating factors, e.g. high protein intake, trauma, intercurrent infections, surgery, childbirth or treatment with sodium valproat [40].

Symptoms in the neonatal period include feeding difficulties, lethargy, respiratory distress, impairment of consciousness, vomiting, convulsions, and coma. Symptoms in the late onset type include headache, vomiting, lethargy, hyperventilation, episodes of abnormal behavior and sometimes disorientation and confusion, ataxia and hypotonia. Acrodermatitis, probably linked to a deficiency of arginine, has also been reported. One particular symptom is a specific anorexia for high protein foods, sometimes leading to the voluntary adoption of a vegetarian diet [40].

The diagnosis should be considered in any patient with unexplained neurological and psychiatric disorders with selective anorexia, and when coma with cerebral oedema and respiratory alkalosis occurs. To confirm the diagnosis the first step is to check for hyperammonaemia, elevated glutamine and alanine, and decreased citrulline plasma

levels and elevated urinary orotic acid and uridine. This can be followed by a liver biopsy to measure the enzyme activity or by mutation analysis [40].

Carbamoyl phosphate is necessary for the removal of ammonia from circulation and glutamate, aspartate, glutamine and asparagine will act as intravascular and intracellular buffers for excess ammonia. There are several possible results of OCTD. The excess of glutamine, whose synthesis is the major pathway for the removal of ammonia in the brain, causes osmotic swelling of the brain. The excess of ammonia also inhibits the enzyme α-ketoglutarate dehydrogenase, critical for pyruvate oxidation, which can lead to loss of ATP and acetylcholin production. Transport of tryptophan across the blood-brain barrier is increased by hyperammonaemia and its metabolite, quinolinic acid, is an excitotoxin. An increased brain content of the excitatory amino acid aspartate could be a reason for the occurrence of seizures [40].

When plasma ammonia levels are found to be elevated, treatment can be given with a low protein diet with supplemental arginine, and with both sodium benzoate and phenylbutyrate to remove excess nitrogen. Acute hyperammonaemia usually requires continuous arteriovenous haemofiltration [40].

Approximately 140 mutations that give rise to OCTD have been identified [49]. Most mutations cause reduced enzyme activity, but some have been identified which do not [40]. Many OTCD mutations are at or near active site. They include K88N, R92Q, T93A, H117L, R141Q/P, N161S, G162R, H168Q, D175V, D196V, D263N, M268T, G269E, T264A, R277W/Q, H302Q/L/Y, C303Y, L304F, and R330G. These mutations directly interfere with substrate binding and/or catalysis. Shi et al. has proposed how several other OCTD mutations can affect the function of OCT (e.g. by helix disruption, interfering with domain closure or folding of protein and affecting of assembly of the trimer) [32].

3 AIM OF THE WORK

This work continued with previous investigations carried out in the LBBCV. The team of this laboratory has demonstrated that glycoxidative damages accumulate in the mitochondrial matrix with aging, in correlation with impairment of this organelle and its functions. Ornithine carbamoyltransferase (OCT), the second enzyme of the urea cycle, has been identified as one of the markedly glycated (respectively carboxymethylated) proteins in senescent rats (27 months old).

The goal of this work was to investigate *in vitro* and *ex vivo* glycation of OCT and the effect of glycation on its function. As a model of glycation, methylglyoxal (MGO), one of the most reactive physiological glycating agents was used. Purified OCT and mitochondrial matrix extracts were incubated with methylglyoxal and submitted to the enzymatic assay and immunochemical analysis. At the same time, the effect of MGO on mitochondrial respiration was observed in order to demonstrate the overall toxicity of this compound.

4 EXPERIMENTAL PART

4.1 MATERIALS AND METHODS

4.1.1 Animals

Experiments were performed on 3 months old male Wistar rats, purchased from Charles River Laboratories (L'Arbresle, France), fed with a standard rodent diet [50]. Water was provided *ad libitum*.

4.1.2 Reagents

- Ornithine transcarbamylase from *Streptococcus faecalis*, lyophilized powder (828 U/mg solid, 1110 U/mg protein), Sigma-Aldrich
- Methylglyoxal, 40 % aqueous solution, Sigma-Aldrich
- Products for SDS-PAGE (10 % SDS solution, 40 % Acrylamide/Bis solution, TEMED), Bio-Rad Laboratories
- Anti-CML antibody, rabbit polyclonal antibody, prepared in the laboratory
- Anti-AGE antibody, mouse monoclonal antibody, clone 6D12, Trans Genic Inc.
- Anti-rabbit IgG, HRP linked whole antibody (from goat), Sigma-Aldrich
- Anti-mouse IgG, HRP linked whole antibody (from sheep), Amersham Biosciences
- Deionized water was prepared by a Millipore System (Milli-RO 5 plus connected with Milli-Q), Millipore
- Other reagents were purchased from Sigma-Aldrich unless otherwise specified

4.1.3 Isolation of Mitochondria

Animals were sacrificed by cervical dislocation without anaesthesia. The removed liver was immediately placed in an ice-cold isolation buffer (0,25 M sucrose, 2 mM EDTA and 25 mM Tris HCl, pH 7,4) and quickly minced. According to Rosca et al. [8], in this buffer, mitochondria could be stored at 4 °C for up to 5 h without a change in the respiratory rates. 10 % tissue homogenate was prepared by using a glass-teflon homogenizer. Unbroken tissue, whole cells, cell debris and nuclei were pelleted by centrifugation at 600 g for 10 min at 4 °C. The supernatant was filtered through two layers of gauze and centrifuged at 8 000 g for 10 min at 4 °C. This yields the mitochondrial pellet. The supernatant was removed, the pellet was resuspended in a

small volume of the isolation buffer and then rinsed in a big volume of this buffer by centrifugation under the same conditions. Finally, the pellet of mitochondria was resuspended in a small volume of the isolation buffer and submitted either to measurement of mitochondrial respiration or frozen for further investigations.

4.1.4 Determination of Protein Concentration

The Bradford method was used to assess the protein content in the samples. This method gives a rapid and accurate determination of protein concentration. It is based on the observation that the maximum absorbance for an acidic solution of Coomassie Brilliant Blue G-250 dye (Bio-Rad Protein Assay, Bio-Rad Laboratories) shifts from 465 to 595 nm when binding to protein occurs. BSA (0 – 12 µg/ml solution) was used as a protein standard, absorbance was recorded at 595 nm. All samples were assayed in duplicate.

4.1.5 Measurements of Mitochondrial Respiration

Mitochondrial respiration was measured using a polarographic Clark electrode (model 1060, Instech Laboratoires). This electrode is composed of a platinum cathode (a pure platinum wire in a fused glass seal) and a silver anode connected by a salt bridge (concentrated KCl solution) and covered by an oxygen permeable polyethylene membrane. Oxygen dissolved in a sample diffuses through the membrane and is reduced at the surface of the cathode. At the same time, AgCl is formed on the surface of the anode and electrical current is produced, proportionally to the rate of dissolved oxygen. The amplifier used with this electrode converts the nanoamp current into a voltage to measure pO_2.

Mitochondria, at a concentration of 0,5 mg/ml, were incubated for varying times in an oxphos buffer (125 mM KCl, 5 mM KH_2PO_4 at pH 7.25) in the presence or absence of 0.59 mM MGO at 37 °C. Time-dependent oxygen consumption was measured every 15 s. State 2 respiration was initiated by adding NADH-linked substrates (10 mM glutamate and 5 mM malate). After stabilization for 2 min in the chamber at 24 °C, ADP (0,625 mM) was added to begin state 3 respiration. After ADP exhaustion, state 4 respiration was monitored. Oxygen consumption was expressed either as nanomoles O_2 per minute per milligram mitochondrial protein, or as a respiratory quotient (state 3/state 4 ratio).

4.1.6 Isolation of Mitochondrial Matrix

Mitochondrial suspensions were frozen at – 80 °C, thawed and exposed to sonic oscillation (10 x 10 s). Deep freezing and sonication ensure the disruption of the membranes. The suspension was centrifuged for 15 min at 15 000 g at 4 °C to remove possibly intact mitochondria. The supernatant was then ultracentrifuged for 45 min at 100 000 g and 4 °C. The resulting supernatant contains the mitochondrial matrix proteins.

4.1.7 Incubation of Mitochondrial Matrix with Methylglyoxal

Mitochondrial matrix extracts were diluted with a carbonate buffer (15 mM Na_2CO_3, 35 mM $NaHCO_3$, pH 8,3) with or without 0,59 mM MGO to a target concentration of 0,2 mg/ml and incubated for various times (0, 5, 15, 30 and 60 min) at 37 °C. These samples were immediately subjected to the OCT activity assay. Each time of incubation was carried out in duplicate, samples from four animals were examined.

Results were expressed as a specific activity (U/mg protein), as a percentage of the initial activity, or as a percentage of the activity of control samples in each time.

4.1.8 Incubation of purified OCT with Methylglyoxal

Ornithine carbamoyltransferase from *Streptococcus faecalis* was diluted with a carbonate buffer with or without 0,59 mM MGO to the target concentration of 1,0 U/ml and incubated at 37 °C. Incubation times were the same as above. These samples were also immediately subjected to the OCT activity assay. For each time of incubation four samples were incubated separately.

Results were expressed as an activity of the enzyme solution (U/ml), as a percentage of the initial activity, or as a percentage of the activity of control samples in each time.

4.1.9 Ornithine CarbamoylTransferase Activity Assay

The OCT activity was measured spectrophotometrically (Kontron Instrument, Uvikon 922) according to the Sigma quality control test procedure for this product. This procedure is based on the determination of the rate of citrulline formed by the enzyme from ornithine and carbamoyl phosphate.

The reaction mixture, in the final volume of 3 ml, contained 7,7 mM Tris HCl at pH 8,5, 5 mM L-ornithine hydrochloride, 5 mM carbamyl phosphate dilithium salt and an appropriate amount of OCT. After incubation at 37 °C for 15 min, the reaction was terminated by the addition of 3 ml 6,25 % (w/v) TCA . 1 ml of the final solution was mixed with 0,25 ml of a redox buffer (0,9 g $NH_4Fe(SO_4)_2$.12 H_2O, 1,1 g $(NH_4)_2Fe(SO_4)_2$.6 H_2O in 10 ml of 1 M H_2SO_4), 1,25 ml of an acid solution (7,4 M H_3PO_4, 3 M H_2SO_4) and 0,5 ml of a diacetyl monoxime solution (75 mM 2,3-butanedione monoxime). Then the samples were incubated in a boiling water bath for 20 min. After cooling to room temperature in a cold water bath, protected from light, 8 ml of deionized water was added and the absorbance at 490 nm was recorded.

The standard curve was obtained by using 1 ml of citrulline solution in deionized water (0 – 8 μmol/ml) and adding all the reagents as described above. For the blank sample, the enzyme (or matrix proteins extract) was added to the reaction mixture after TCA.

One unit of OCT activity was defined as the amount of the enzyme, which catalyzes the formation of 1 μmole of citrulline per minute at 37 °C under standard assay conditions.

$$Activity\ [U/ml] = \frac{[\mu moles\ of\ citrulline] \times V_R}{t \times V_S}$$

Figure 16. Calculation of OCT activity [U/ml of enzymatic solution]. [μmoles of citrulline] were determined from the standard curve, V_R – reaction volume (6 ml), t – time (15 min), V_S – sample volume (0,1 ml)

$$Activity\ [U/mg] = \frac{[\mu moles\ of\ citrulline] \times V_R}{t \times m}$$

Figure 17. Calculation of OCT specific activity [U/mg protein]. [μmoles of citrulline] were determined from the standard curve, V_R – reaction volume (6 ml), t – time (15 min), m – mg of protein subjected to the reaction (in 0,1 ml of the sample)

4.1.10 Preparation of the samples for SDS-PAGE and WB Analysis

Purified OCT (1 μg) and mitochondrial matrix proteins (20 μg for SDS-PAGE or 10 μg for WB) were incubated for various times (30 min, 120 min, 24 h) in the carbonate buffer (see 4.1.7) in the presence of 0,59 mM methylglyoxal at 37 °C. In order to stop the reaction with methylglyoxal, 3 volumes of cold ethanol (-20 °C)

were added to the samples and after 15 min at -20 °C, the proteins were pelleted by centrifugation at 10 000 g and 4 °C for 10 min. The supernatant was discarded and its residues were evaporated using a centrifugal evaporator. The final pellet was mixed with the sample buffer (62,5 mM Tris HCl pH 6,8, 2 % SDS, 10 % glycerol, 100 mM β-ME, 0,001 % bromophenol blue) and boiled for 5 min at 100 °C.

Control samples were prepared by the same procedure without methylglyoxal. Bovine serum albumin modified by glyoxal, i.e. carboxymethylated BSA (CML-BSA) (1 μg for SDS-PAGE or 0,1 μg for WB), directly mixed with the sample buffer, was used as a positive control.

4.1.11 SDS-PAGE

Electrophoresis is the migration of charged molecules in a solution under an electric field. In SDS-PAGE (Sodium dodecyl sulphate polyacrylamide gel electrophoresis) separation, migration is not determined by an intrinsic electric charge of polypeptides but by molecular weight. SDS is an anionic detergent that denatures proteins by binding around the polypeptide backbone in a constant mass ratio. So doing, SDS confers a negative charge to a polypeptide in proportion to its weight. The proteins are usually entirely unfolded by reducing the disulfide bridges with dithiothreitol (DTT) or with β-mercaptoethanol (β-ME). Acrylamide polymerizes to a porous gel, which acts as a sieve by retarding or obstructing the movement of large polypeptides towards the anode, allowing the smaller ones to migrate freely. SDS-PAGE is useful for separation of a protein (e.g. before the Western blotting procedure), for determining its relative abundance in the sample and its approximate molecular weight. Protein fragmentation or cross-linking can be detected as well. Different staining methods are used to visualize the proteins (e.g. Coomassie Brilliant Blue-, copper or silver staining).

Separation of proteins was carried out using the Mini-PROTEAN 3 Electrophoresis System (Bio-Rad Laboratories). Stacking polyacrylamide gel was 3 % (5,0 ml of deionized water, 1,87 ml of 0,5 M Tris HCl pH 6,8, 75 μl of 10 % SDS, 0,6 ml of 40 % acrylamide, 150 μl of 10 % APS and 10 μl of TEMED) and the resolving gel was 10 % (12,7 ml of deionized water, 6,56 ml of 1,5 M Tris HCl pH 8,8, 262,5 μl of 10 % SDS, 6,6 ml of 40 % acrylamide, 300 μl of 10 % APS and 20 μl of TEMED). Electrophoretic migration was performed in the running buffer (25 mM Tris, 192 mM glycine, 0,1 % SDS) at a constant current of 30 mA per gel. Proteins were

detected by Coomassie blue staining (0,25 % (w/v) Coomassie Brilliant Blue R-250, 45 % (v/v) ethanol, 10 % (v/v) acetic acid) or transferred to a nitrocellulose membrane for further investigations. Precision Plus Protein All Blue Standards (Bio-Rad Laboratories) were used as molecular weight standards.

4.1.12 Western Blotting Analysis

The blotting procedure combines the resolution of gel electrophoresis with the specificity of immunological detection. It usually involves an electrophoretic transfer of proteins to a membrane (Western blotting), followed by blockade (saturation) of remaining non-specific binding sites, indirect immunoassay and detection. Proteins are "blotted" to the membrane (e.g. nitrocellulose, nylon or PVDF) to render them accessible for probing. Saturation is done with a concentrated protein solution (BSA or non-fat milk powder). The membrane is then incubated in the primary (antigen-specific) and subsequently in the secondary (first antibody-directed) antibody solution. The latter is ordinarily enzyme-labelled and the nature of label (e.g. horseradish peroxidase, alkaline phosphatase) in combination with the substrate used predetermines the detection method. The most common is colorimetric or chemiluminescent detection. Western blotting immunoanalysis provides both qualitative and quantitative information about the antigen and can be the follow-up to both one-dimensional and two-dimensional electrophoresis.

After SDS-PAGE, the mitochondrial proteins were electroblotted to a nitrocellulose membrane (Hybond-C Extra, Amersham Biosciences) for 90 min at 100 V using the Mini Trans-Blot Module (Bio-Rad Laboratories). Transfer was performed in a buffer containing 25 mM Tris pH 8,3, 192 mM glycine, 20 % ethanol and was verified by Red Ponceau-S staining. The membrane was saturated with PBS, 0,1 % (v/v) Tween 20, 1 % (w/v) BSA overnight at 4 °C and washed three times for 10 min with a washing buffer (PBS, 0,2 % (v/v) Tween 20). Then the membrane was incubated either with polyclonal anti-CML antibody (dilution 1/1 000) or with monoclonal anti-AGE antibody (dilution 1/3 000) for 90 min. The membrane was washed as above and incubated with the secondary HRP linked antibodies for 60 min: anti-rabbit IgG (dilution 1/20 000) against the anti-CML antibody and anti-mouse IgG (dilution 1/20 000) against the anti-AGE antibody. All antibodies were diluted in PBS, 0,1 % (v/v) Tween 20 and incubations were performed at room temperature. Finally,

the membranes were washed three times for 20 min in the washing buffer and proteins were revealed by SuperSignal West Pico Chemiluminiscent Substrate (Pierce) (WP) or by Amersham ECL Advance Western Blotting Detection Kit (GE Healthcare) (AWB). The arising chemiluminiscent signal was captured on photographic film (Hyperfilm-ECL, Amersham Biosciences).

4.2 RESULTS

4.2.1 OCT *in vitro* Activity

Purified OCT from *Streptococcus faecalis* (0,90 µg/ml that corresponds to 1,0 U/ml) was incubated with or without 0,59 mM MGO at 37 °C for various times (0, 5, 15, 30 and 60 min). For each time of incubation four samples were incubated separately. The enzymatic activity of the samples was determined according to the OCT activity assay procedure (see 4.1.9) and the data was expressed as an activity of the enzyme solution (U/ml) (Table 3 and Table 4). Control activity at zero time of incubation (initial activity) was 0,955 ± 0,028 U/ml. The Figure 18 shows a decline of OCT activity as a function of time.

Activity [U/ml]

min	MGO 0,59 mM				Control			
0	0,928	0,690	0,637	0,607	0,909	0,969	0,983	0,957
5	0,644	0,616	0,610	0,544	0,761	0,742	0,754	0,862
15	0,464	0,506	0,501	0,440	0,647	0,703	0,696	0,676
30	0,370	0,359	0,348	0,307	0,660	0,585	0,615	0,632
60	0,209	0,207	0,197	0,189	0,654	0,683	0,637	0,556

Table 3. Activity of OCT in the presence of 0,59 mM MGO at different times of incubation. Values of 4 different experiments

Activity [U/ml]

min	MGO 0,59 mM	Control	
0	0,716 ± 0,126	0,955 ± 0,028	*
5	0,604 ± 0,036	0,780 ± 0,048	**
15	0,478 ± 0,027	0,680 ± 0,022	**
30	0,346 ± 0,024	0,623 ± 0,027	**
60	0,201 ± 0,008	0,633 ± 0,047	**

Table 4. Activity of OCT in the presence of 0,59 mM MGO at different times of incubation. Means of the values from the Table 3 ± SD. */** significant difference between treated and untreated samples in each time of incubation according to the Student's t-test, * $p < 0,05$ ** $p < 0,01$

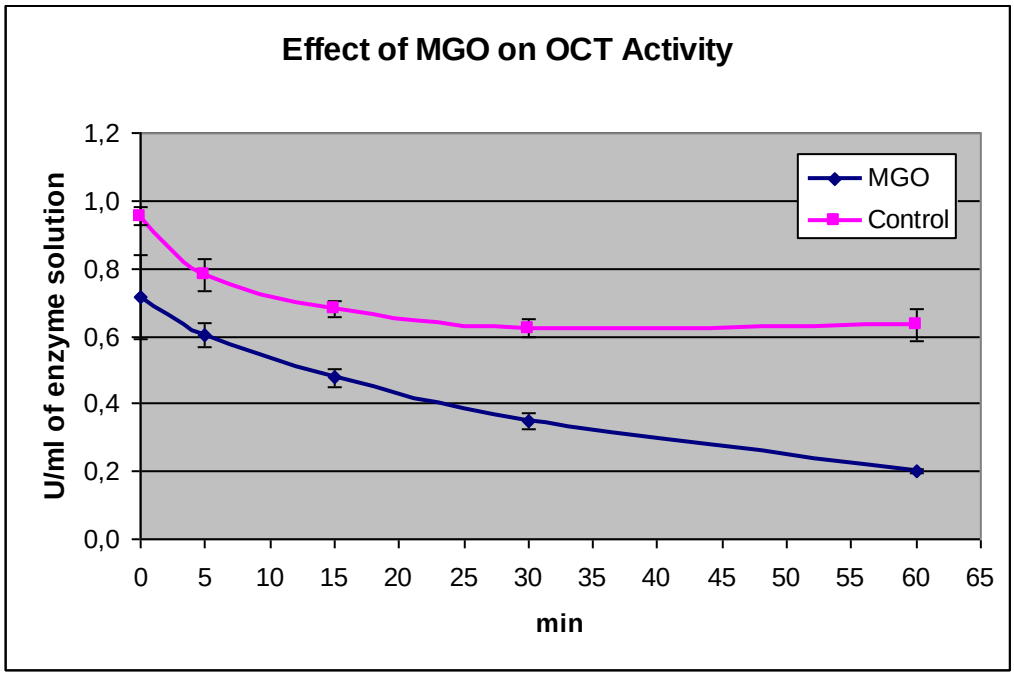

Figure 18. Activity of OCT in the presence or absence of 0,59 mM MGO as a function of time

To compare the values of activity at different times, the data was expressed as a percentage of the initial activity (Table 5 and Figure 19). We observed a significant decline in the activity of the control samples with time: after 60 min of incubation the activity fell to 66,3 ± 5,0 %. The harmful effect of 0,59 mM methylglyoxal on OCT activity is evident even at the zero time of incubation: 75,0 ± 13,2 % of control activity, while after 60 min the activity fell to 21,0 ± 0,8 %. According to the Student's t-test the samples treated with MGO exhibit significantly different activity ($p < 0,05$ at zero time of incubation and $p < 0,01$ for the rest).

% of initial activity

min	MGO 0,59 mM	Control
0	75,0 ± 13,2	100,0 ± 2,9
5	63,2 ± 3,8	81,7 ± 5,0
15	50,0 ± 2,9	71,3 ± 2,3
30	36,2 ± 2,5	65,3 ± 2,9
60	21,0 ± 0,8	66,3 ± 5,0

Table 5. Effect of MGO on OCT activity at different times of incubation. Data is expressed as a percentage of the initial activity (n = 4)

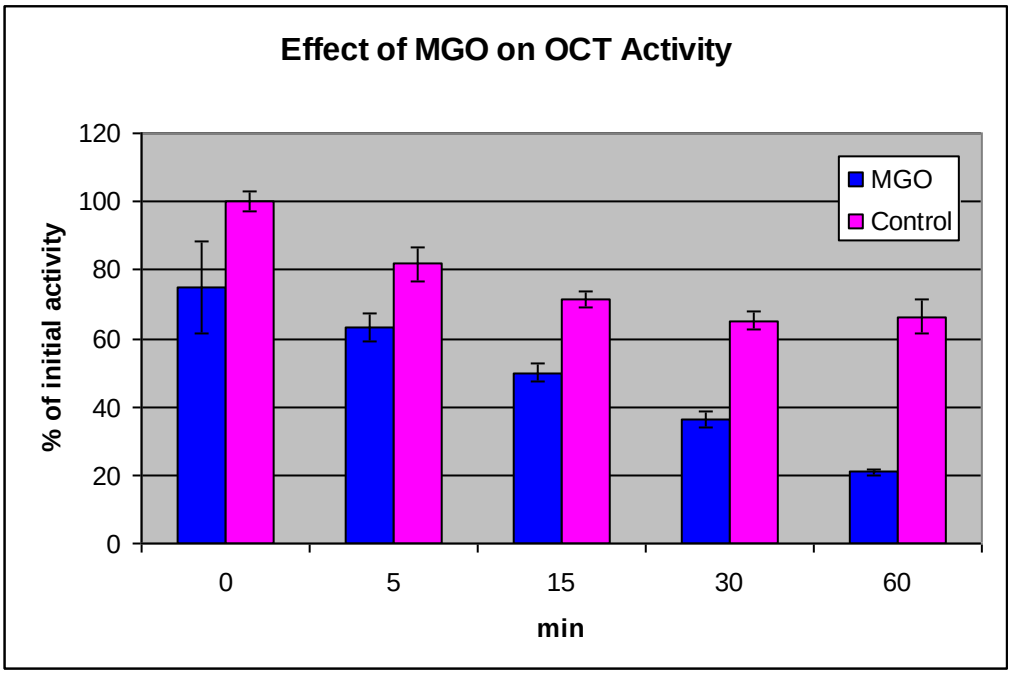

Figure 19. Effect of 0,59 mM MGO on OCT activity at different times of incubation. Data is expressed as a percentage of the initial activity (n = 4)

In order to evaluate the difference in activity between the control samples and those treated with methylglyoxal, the activity was expressed as a percentage of the control activity in each time of incubation (Table 6 and Figure 20). In the first 15 min of incubation the treated samples had around 70 % of the control activity, while after 60 min only around 30 % of the control activity.

% of control activity

min	MGO 0,59 mM	Control
0	75,0 ± 13,2	100,0 ± 2,9
5	77,4 ± 4,7	100,0 ± 6,2
15	70,2 ± 4,0	100,0 ± 3,2
30	55,5 ± 3,8	100,0 ± 4,4
60	31,7 ± 1,2	100,0 ± 7,5

Table 6. Effect of MGO on OCT activity at different times of incubation. Data is expressed as a percentage of the control activity at each time of incubation (n = 4)

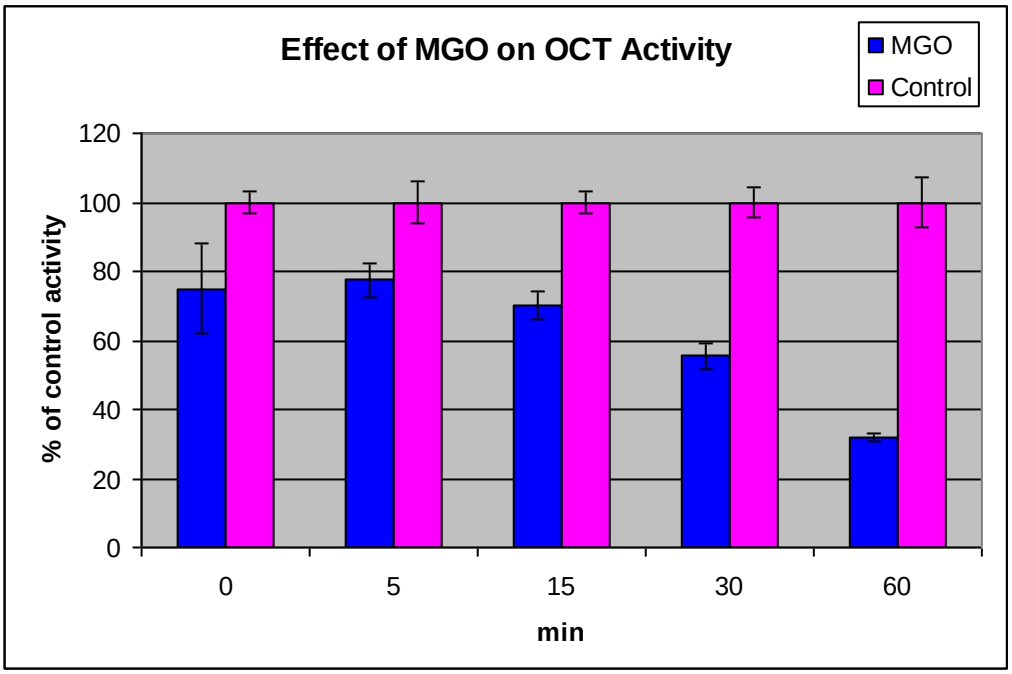

Figure 20. Effect of 0,59 mM MGO on OCT activity at different times of incubations. Data is expressed as a percentage of the control activity at each time of incubation (n = 4)

4.2.2 OCT *ex vivo* Activity

Mitochondrial matrix proteins (0,2 mg/ml) from young animals were incubated for various times (0, 5, 15, 30 and 60 min) at 37 °C with or without 0,59 mM MGO. Each time of incubation of each sample was carried out in duplicate. The OCT-like activity of the samples was determined according to the OCT activity assay procedure (see 4.1.9) and the data was expressed as specific activity of the matrix extracts (U/mg protein) (Table 7 and Table 8). Control activity at zero time of incubation (initial activity) was 4,981 ± 0,617 U/mg protein. The Figure 21 shows a decline of OCT-like activity as a function of time.

Specific activity [U / mg]

min	MGO 0,59 mM				Control			
0	5,081	3,865	4,321	5,247	5,496	4,273	4,471	5,686
5	1,441	1,268	1,234	1,302	4,853	3,928	4,589	5,031
15	0,394	0,454	0,426	0,426	5,008	3,980	4,695	5,069
30	0,239	0,241	0,210	0,216	4,825	3,891	4,103	4,700
60		0,151	0,093	0,162	4,338	3,371	3,719	4,174

Table 7. OCT-like activity in the presence of 0,59 mM MGO at different times of incubation. Values of activity of samples from 4 different animals, each experiment was performed in duplicate

Specific activity [U / mg]

min	MGO 0,59 mM	Control	
0	4,629 ± 0,562	4,981 ± 0,617	
5	1,311 ± 0,079	4,600 ± 0,419	**
15	0,425 ± 0,021	4,688 ± 0,433	**
30	0,227 ± 0,014	4,380 ± 0,392	**
60	0,135 ± 0,030	3,901 ± 0,381	**

Table 8. OCT-like activity in the presence of 0,59 mM MGO at the different times of incubation. Means of values from the Table 7 ± SD. ** significant difference between treated and untreated samples at each time of incubaion according to the Student's t-test, $p < 0,01$

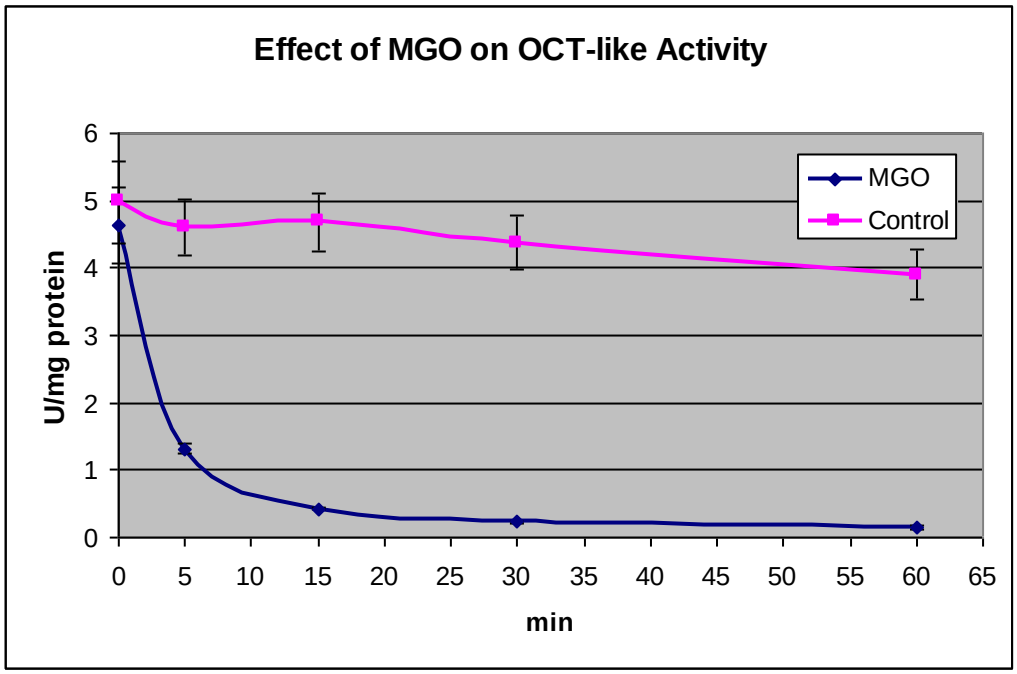

Figure 21. OCT-like activity in the presence of 0,59 mM MGO as a function of time

To compare the values of activity at different times, the data was expressed as a percentage of the initial activity (Table 9 and Figure 22). We observed a slight decline in the activity of the control samples: after 60 min of incubation the activity decreased to 78,3 ± 7,6 %. At the zero time of incubation OCT-like activity of the samples treated with 0,59 mM methylglyoxal was not significantly different: 92,9 ± 11,3 % of control activity. Conversely, after 5 min of incubation the activity of treated samples fell to 26,3 ± 1,6 % and to 2,7 ± 0,6 % after 60 min. According to the Student's t-test, the samples incubated for 5 to 60 min with methylglyoxal exhibit significantly different activity ($p < 0,01$).

% of initial activity

min	MGO 0,59 mM	Control
0	92,9 ± 11,3	100,0 ± 12,4
5	26,3 ± 1,6	92,3 ± 8,4
15	8,5 ± 0,4	94,1 ± 8,7
30	4,5 ± 0,3	87,9 ± 7,9
60	2,7 ± 0,6	78,3 ± 7,6

Table 9. Effect of MGO on OCT-like activity at different times of incubation. Data is expressed as a percentage of the initial activity (n = 4)

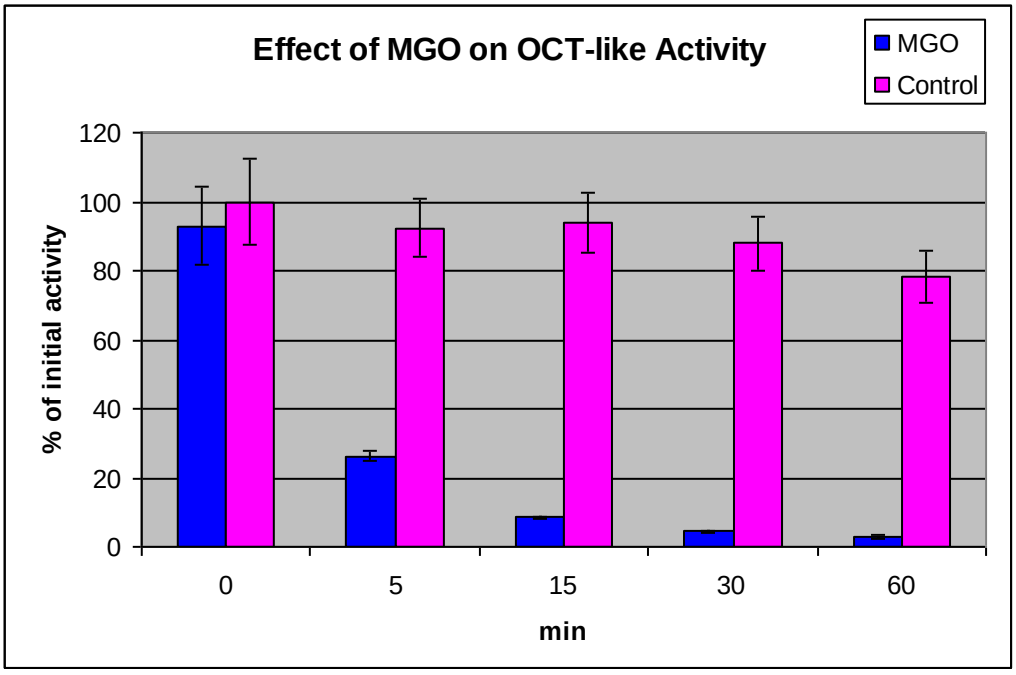

Figure 22. Effect of 0,59 mM MGO on OCT-like activity at different times of incubation. Data is expressed as a percentage of the initial activity (n = 4)

In order to evaluate the difference in activity between the control samples and those treated with methylglyoxal, the activity was expressed as a percentage of the control activity at each time of incubation (Table 10 and Figure 23). After 5 min of incubation the treated samples had only around 30 % of the control activity and after 60 min this activity barely represented 3 % of the control activity.

% of control activity

min	MGO 0,59 mM	Control
0	92,9 ± 11,3	100,0 ± 12,4
5	28,5 ± 1,7	100,0 ± 9,1
15	9,1 ± 0,5	100,0 ± 9,2
30	5,2 ± 0,3	100,0 ± 9,0
60	3,5 ± 0,8	100,0 ± 9,8

Table 10. Effect of MGO on OCT-like activity in different times of incubation. Data is expressed as a percentage of the control activity (n = 4)

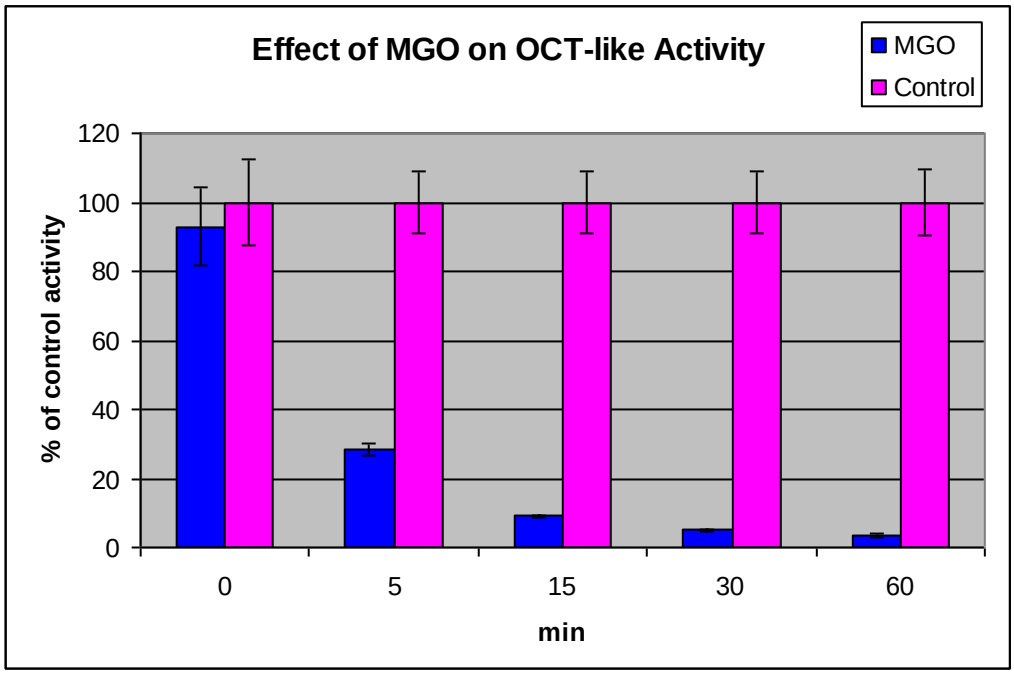

Figure 23. Effect of 0,59 mM MGO on OCT-like activity in different times of incubation. Data is expressed as a percentage of the control activity in each time of incubation (n = 4)

4.2.3 SDS-PAGE and Western Blotting Analysis

In order to investigate *in vitro* and *ex vivo* glycation of OCT, the SDS-PAGE followed by immunochemical analysis was carried out. Purified OCT from *Streptococcus faecalis* and samples of mitochondrial matrix proteins were incubated for various times with methylglyoxal (see 4.1.10). Because of unavailable anti-OCT antibody, each time purified OCT and the mitochondrial matrix proteins were run on the same gel to attempt to localize this enzyme among the other proteins. To assess the content of glycated proteins, polyclonal anti-CML antibody and monoclonal anti-AGE antibody were used. CML-BSA served as a positive control.

An example of Coomassie blue stained gel with control or MGO-treated samples of OCT and mitochondrial proteins is shown (Figure 24). Control OCT appears as a single band between 50 and 37 kDa. Supposing that Rf is a function of log MW (Da), this band corresponds to the MW of 43 kDa. In the lanes with OCT incubated with MGO for 30 and 120 min, the main band is significantly less intensive, while a band between 100 and 75 kDa appears, which corresponds to the dimer of this enzyme. There are also visible traces of high-molecular protein complexes (MW > 250 kDa) suggesting the formation of the cross-links. After incubation for 24 h with MGO, the main band becomes poorly visible while high-molecular complexes seem to be more apparent.

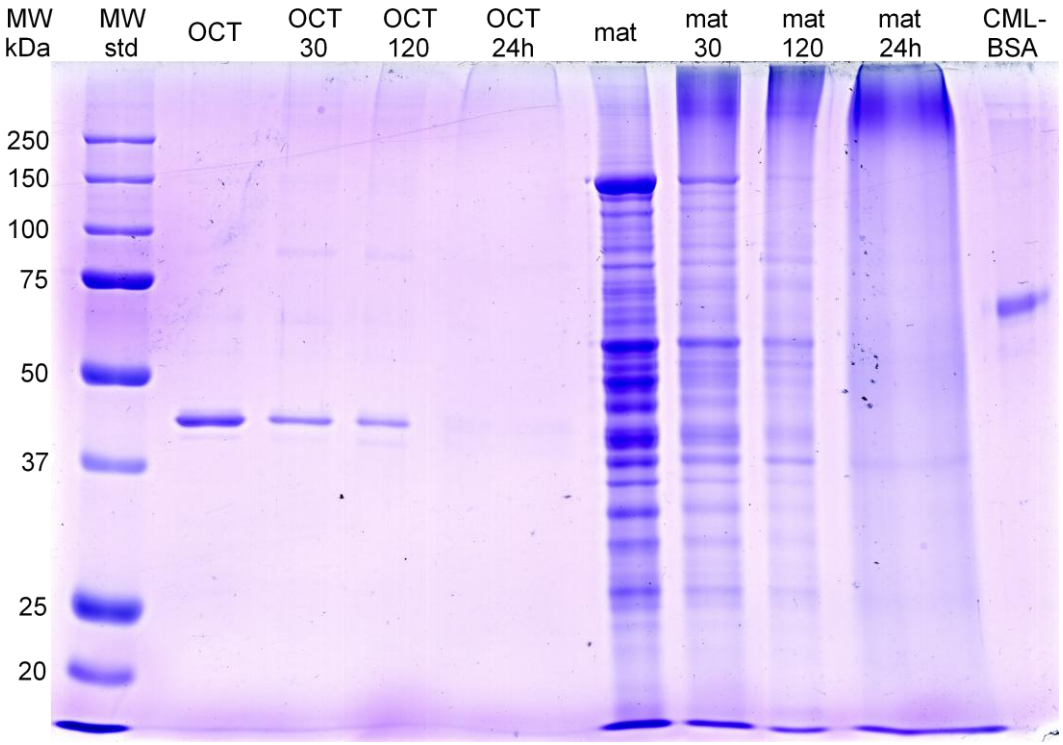

Figure 24. Samples of purified OCT and mitochondrial matrix proteins treated with 0,59 mM MGO separated by SDS-PAGE, Coomassie blue stain. OCT = OCT from *Streptococcus faecalis* (1 µg/lane), mat = mitochondrial matrix proteins (20 µg/lane), number = time of incubation (min), CML-BSA = positive control of glycated proteins (1 µg/lane)

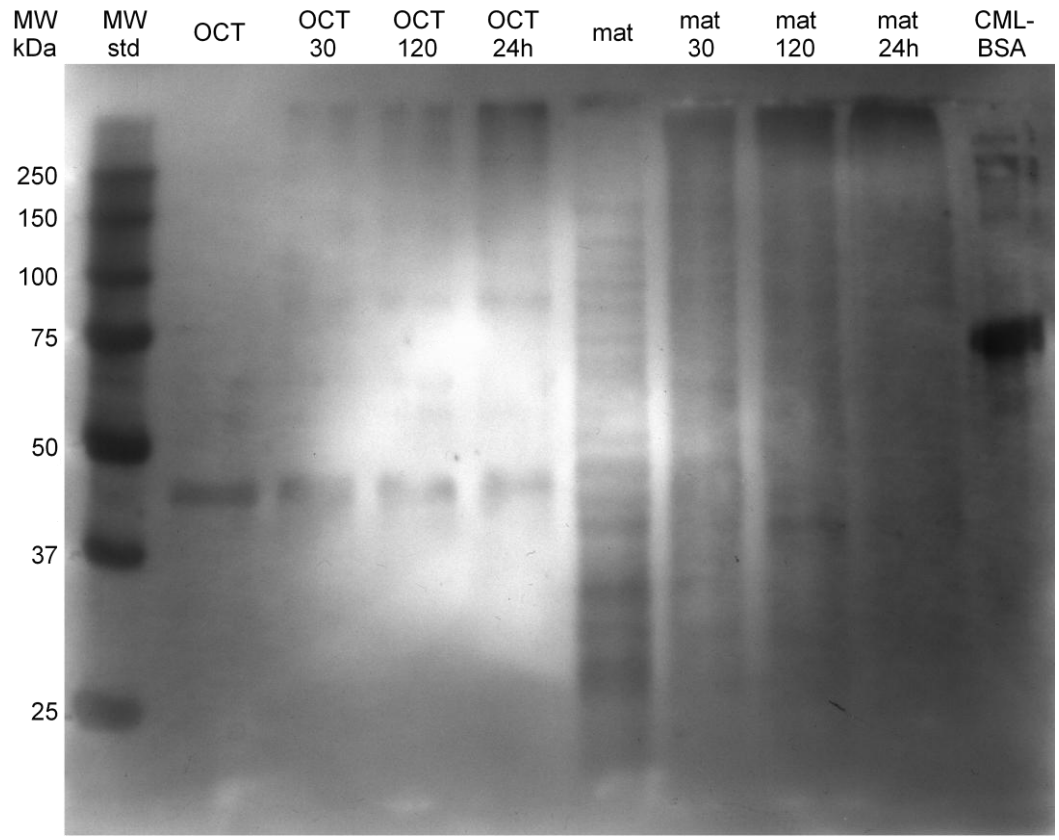

Figure 25. Western blotting analysis with polyclonal anti-CML antibody. Samples and legend identical with the Figure 24, revealed by WP

This phenomenon was observed on the other Coomassie blue stained gels prepared by the same procedure.

In the lane with control matrix proteins, there is around 30 well separated more or less intensive protein bands, in the high molecular fraction (above 250 kDa) there seems to be a minimum of total protein amount. In the lane with matrix proteins incubated for 30 min with MGO, the same pattern of the protein bands is observed, but all the bands are considerably less intensive, while in the high molecular fraction a significant amount of proteins appears. This phenomenon is more pronounced after 120 min of incubation, where some of the protein bands from the control pattern disappeared and some of them became hardly distinguishable. In the lane with the matrix proteins treated with MGO for 24 h, there is only one visible protein band, while the bulk of proteins are accumulated in the high molecular weight fraction.

Proteins from another gel, run under the same conditions, were electroblotted to a nitrocellulose membrane and subjected to the immunochemical analysis with polyclonal anti-CML antibody (Figure 25). Unfortunately, the antibody has a high non-specific reaction with the saturating agent BSA (this fact explains the dark background of the membrane). Nevertheless, practically constant labelling of the OCT main band can be observed in each lane with purified OCT. In the lanes with OCT treated with MGO, its dimers and high-molecular complexes are clearly visible, not surprisingly, most pronounced after 24 h of incubation. The labelling of the CML-BSA is also evident, showing its main band around 70 kDa and several traces of higher molecular mass complexes.

In the lane with control matrix proteins, some protein bands are clearly visible in the whole spectrum of MW, but labelling of the bands of lower molecular weight seems to be more intensive. The pattern of the bands is different than that one observed by Coomassie blue staining. This fact confirms that the labelling by the antibody is not completely non-specific. In the lanes with matrix proteins treated with MGO, almost no bands can be recognized. The entire lane has almost the same level of labelling (more intensive that the background of control lane), only in the high molecular fraction the labelling is stronger.

The Figure 26 shows an immunochemical analysis with monoclonal anti-AGE antibody. The lanes with OCT exhibit no labelling. In the lane with control matrix proteins there are several visible bands: one close to 150 kDa, one between 75 and 50 kDa, one strong band between 50 and 37 kDa and several slightly visible bands

between 75 and 37 kDa. In the lane with matrix proteins incubated with MGO for 30 min, the same bands are recognized, considerably more intensive, and 4 new bands appear between 150 and 50 kDa. In the lanes with matrix proteins treated for 120 min and 24 h, no specific bands are recognized, the only labelling is of the high-molecular complexes. A strong response to CML-BSA (0,1 μg) and its complexes can be observed.

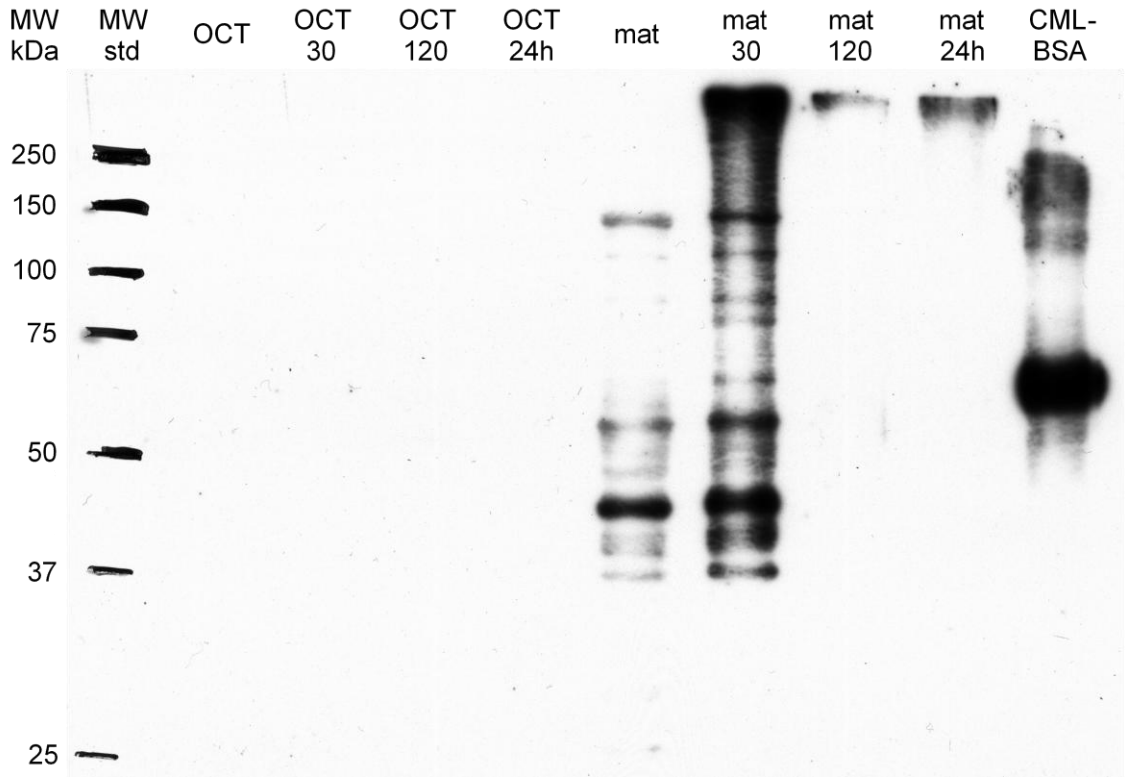

Figure 26. Western blotting analysis with monoclonal anti-AGE antibody. Samples and legend identical with the Figure 24, except for the quantity of matrix proteins (10 μg/lane) and CML-BSA (0,1 μg/lane), revealed by WP

In order to amplify the slight labelling of OCT, the same membrane was revealed by a more sensitive detection kit (AWB), which is able to detect femtograms of HRP (Figure 27). In all OCT lanes, the main band was detected with decreasing intensity. In the lanes with OCT treated with MGO for 30 min and 24 h, there is slightly visible band corresponding to its dimer. In the lanes with treated OCT for 30 and 120 min, high-molecular complexes can be observed. In all the lanes with OCT there are two bands between 75 and 50 kDa of unknown origin.

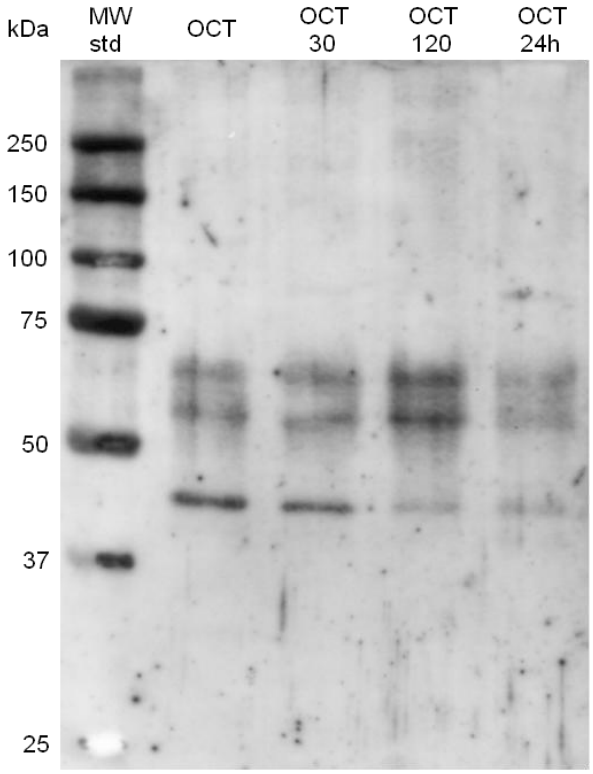

Figure 27. Western blotting analysis with monoclonal anti-AGE antibody. The same membrane as in the Figure 26, excised part with OCT samples, revealed by AWB

4.2.4 Measurements of Mitochondrial Respiration

Isolated mitochondria were incubated in the presence or absence of 0,59 mM MGO for various times at 37 °C and the oxygen consumption during the respiratory states 2, 3 and 4 was monitored by a Clark electrode (see 4.1.5).

Examples of the experiments are shown (Figure 28). In the control mitochondria, we can observe a typical increase in oxygen consumption after the adding of ADP (state 3 respiration, coupled state) and after the ADP exhaustion return to the state 4 respiration (which corresponds to the state 2). This increase is visibly smaller in the mitochondria incubated for 15 min in MGO: the respiration is less effective.

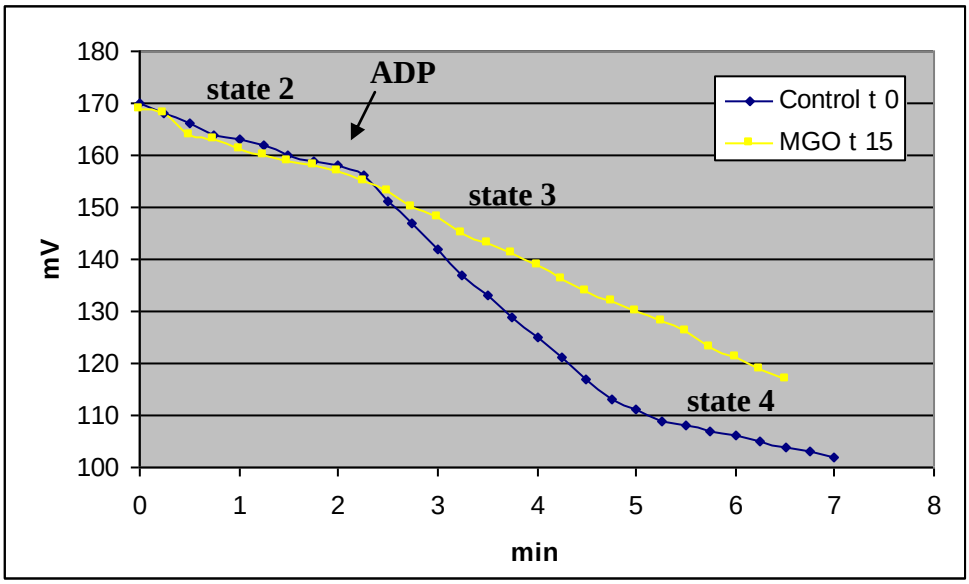

Figure 28. Oxygen consumption by the mitochondria. Electrical potential corresponding to pO_2 was recorded by the Clark electrode during the experiment. State 2 respiration was initiated by adding glutamate and malate, after 2 min ADP was added to begin state 3 respiration, after ADP exhaustion state 4 respiration was monitored. Control t 0 – untreated mitochondria, MGO t 15 – mitochondria incubated with 0,59 MGO for 15 min at 37 °C

Oxygen consumption and respiratory quotient in various conditions are shown (Table 11, Figure 29 and Figure 30). The control mitochondria without incubation at 37 °C had a state 4 respiratory rate of 44,4 nmol O_2/mg/min, after 5 and 15 min of incubation this rate was slightly higher, around 48 nmol O_2/mg/min. Mitochondria incubated for 0 and 5 min with MGO had a state 4 respiratory rate of 51,1 nmol O_2/mg/min and this rate wasn't markedly changed after incubation for 15 min.

State 3 respiratory rates after 0 and 5 min of incubation with MGO kept around 190 nmol O_2/mg/min. Control mitochondria without incubation had the rate slightly lower (177,8 nmol O_2/mg/min) and after 5 min of incubation slightly higher (208,9 nmol O_2/mg/min). After 15 min of incubation, the rate of treated and untreated mitochondria fell to approximately 90 nmol O_2/mg/min, the mitochondria treated with MGO had the consumption slightly higher.

Oxygen consumption [nmol O_2/mg/min]						
	state 4		state 3		Respiratory quotient	
min	MGO	Control	MGO	Control	MGO	Control
0	51,1	44,4	191,5	177,8	3,75	4,22
5	51,1	48,2	191,5	208,9	3,75	4,34
15	51,4	47,6	93,0	88,8	1,82	1,87

Table 11. Oxygen consumption by the mitochondria after incubation with or without 0,59 mM MGO for various times.

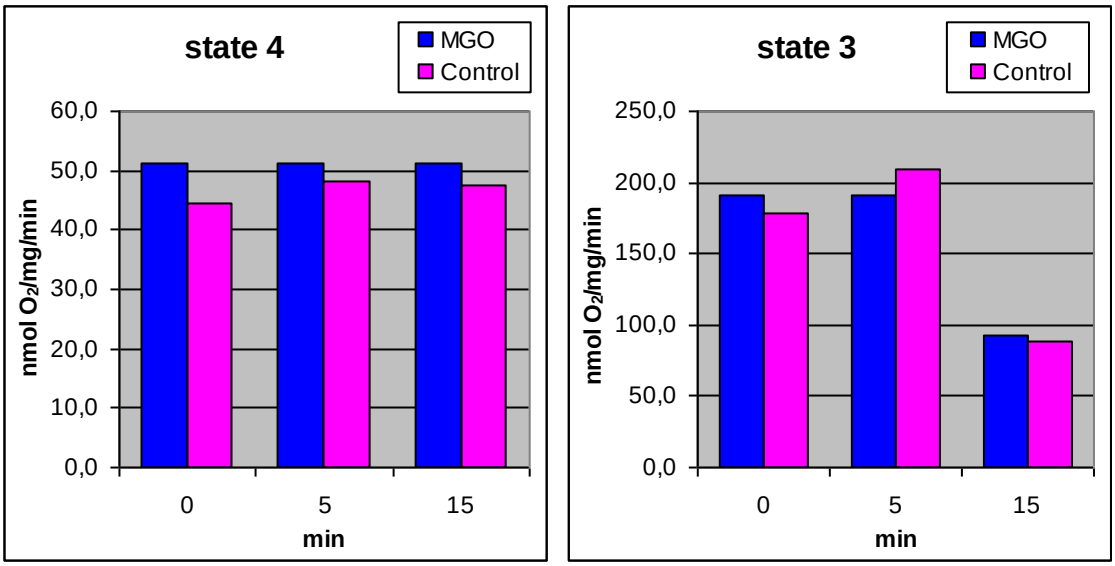

Figure 29. State 4 and state 3 respiration in the presence or absence of MGO. Samples of mitochondrial suspension were incubated for various times in the presence or absence of 0,59 mM MGO at 37 °C.

At all times of incubation, the respiratory quotient is slightly lower in mitochondria treated with MGO (Table 11 and Figure 30), the respiration is less effective than in control mitochondria.

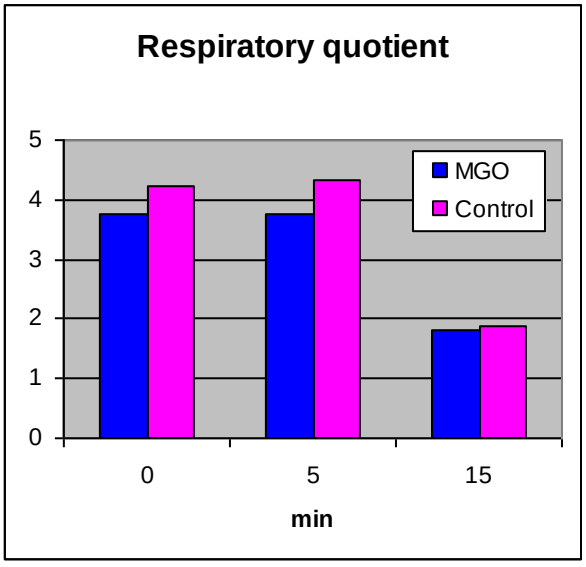

Figure 30. Respiratory quotient of mitochondria incubated with MGO for various times and control mitochondria. Respiratory quotient is a state 3/state 4 respiration ratio.

5 DISCUSSION

The goal of this work was to investigate whether glycation-modification of OCT, evidenced *in vivo* study, affects its activity. For this purpose we used methylglyoxal as a glycating agent in *in vitro* and *ex vivo* approach. The effect of MGO on mitochondrial respiration was also investigated.

MGO is one of the most reactive glycating agents occurring *in vivo*. According to some authors [8], it is the major source of intracellular and plasma AGEs. In comparison with other glycating agents, the protein modification by MGO is a rapid method, giving significant results even after relatively short times of incubation and low concentrations of the agent. Physiologic concentration of free MGO within the living cell is considered < 5 μM [7], but the total concentration of MGO (free and protein-bound) is much higher. There is an evidence for the concentration of MGO as high as 310 μM in cultured Chinese hamster ovary cells [11]. For our experiments, we used 590 μM MGO as a model of glycative conditions.

Samples of purified OCT from *Streptococcus faecalis* or matrix proteins from rat liver mitochondria were incubated with MGO for various times (0, 5, 15, 30 and 60 min) and then subjected to the enzymatic reaction. The activity of OCT was measured spectrophotometrically, using the reaction of citrulline (the product of the enzymatic reaction) with diacetyl monoxime, resulting in orange coloured complexes.

In vitro experiments demonstrated rapid and extensive inactivation of OCT by methylglyoxal. We observed a gradual decline in OCT activity with the time of incubation. After 60 min of incubation with MGO, OCT activity fell to ca 30 % of the control activity. These experiments were carried out in 4 independent samples for each time of incubation, the amount sufficient for statistical analyses. There is a significant difference ($p < 0,05$) between treated and untreated samples even at zero time of incubation: treated samples had ca 75 % of the activity of untreated samples. This fact suggests that the modification of the enzyme is started immediately in the presence of MGO. In fact, MGO had an influence on the enzyme not only during the incubation time, but also during the enzymatic reaction (another 15 min), where MGO was already diluted 1:30. Nevertheless, the fact that MGO has a high affinity to this enzyme is evident. After 5 min of incubation, the statistical difference between treated and untreated samples is even more significant ($p < 0,01$).

Ex vivo experiments showed slightly different development of enzyme inactivation by MGO. While the activities of treated and untreated samples were not

significantly different at zero time of incubation, after 60 min of incubation with MGO, we observed almost complete loss of OCT activity: only ca 3 % of the control activity. These experiments were performed on samples from 4 animals, in duplicate for each time of incubation, i.e. data sufficient for statistical analyses. The significant difference ($p < 0,01$) between treated and untreated samples was observed after 5 min of incubation with MGO, where activity of treated samples fell to ca 30 % of control activity. These data confirm the rapid and extensive inactivation of OCT by methylglyoxal observed *in vitro*.

We can merely speculate about the reason for the difference between *in vitro* and *ex vivo* rapidity of the enzyme inactivation. It can be caused by the structural differences between OCT from *S. faecalis* and rat, by the influence of other compounds present in mitochondrial matrix extracts or by another reason. Theoretically, other proteins present in the mitochondrial matrix, modified by MGO, can create new reactive compounds or cross-links with OCT, blocking its enzymatic function. On the other hand, the presence of other proteins in the mitochondrial matrix can behave as a "buffer" for MGO, causing a later onset of OCT inactivation observed *ex vivo*.

Probably, the main reason of OCT inactivation is the modification of Arg and Lys residues in the active site. According to the detailed studies of OCT structure [32], there are 3 Arg residues (R92, R141 and R330) and one Lys residue (K88) in the active site. The Arg residues directly bind the leading substrate CP and the Lys residue binds ornithine, the second substrate, indirectly through one molecule of water.

The modification of OCT and other mitochondrial matrix proteins by MGO was investigated using SDS-PAGE and Western blotting analysis. The samples of purified OCT from *S. faecalis* and mitochondrial matrix extracts, incubated for various times (0, 30, 120 min and 24 h) with MGO, were separated by polyacrylamide gel electrophoresis and stained by Coomassie blue or subjected to the immunochemical analysis with polyclonal anti-CML or monoclonal anti-AGE antibody.

Surprisingly, the band corresponding to the purified OCT appeared around 43 kDa (while it should be around 38 kDa) in Coomasie blue stained gel and its intensity is significantly lower after incubation with MGO for 30 or 120 min, while after 24 h of incubation, this band is barely visible. This could be explained by the fact, that methylglyoxal is able to form cross-links between the molecules, resulting in the dimers, trimers and high molecular weight complexes of this enzyme. Indeed, bands

corresponding to these products are observable in the gel. Probably, complexes too big to enter the gel are formed, so it seems that most of the protein amount disappeared from the lane.

The same phenomenon appears in the lanes with mitochondrial matrix extracts. With extending the time of incubation with MGO, the intensity of protein bands is lowering, which results in one great bulk of protein complexes of high molecular weight after 24 h of incubation. Comparing the patterns of lanes with proteins incubated for different times, it seems that some proteins are more susceptible to disappear, i.e. to form the cross-links. In the lane with CML-BSA, the formation of bigger complexes is also visible.

There is visible some non-specific labelling of proteins (MW standards and untreated OCT) on the membrane treated with polyclonal anti-CML antibody. Nevertheless, the labelling revealed the main band in all lanes with OCT and highlights the cross-link formation between the molecules of this enzyme. Even untreated mitochondrial matrix proteins are labelled, due to non-specific reaction or more probably to glycation *in vivo*, even at young age, as demonstrated in previous study [2]. The proteins of lower molecular weight seem to be more labelled. The signal is generally more intensive in the lanes with treated matrix, but no specific bands are visible. Great molecular complexes are accumulating with the time of incubation.

Treating the membrane with monoclonal anti-AGE antibody revealed no signal in the lanes with OCT. In the lane with untreated matrix several bands are labelled, suggesting the glycation *in vivo* in young age. Greater set of bands is significantly more labelled in the lane with matrix proteins incubated with MGO for 30 min, with a strong signal of the high molecular weight complexes. Interestingly, no signal is detected after 120 min and 24 h of incubation, except for the slight labelling of the high MW complexes. It seems, that once a protein is modified by MGO (or another glycating agent), it is highly susceptible to form a cross-link with another protein. The results of anti-AGE antibody labelling of OCT, detected by more sensitive detection kit, are comparable to those obtained with anti-CML antibody.

Probably, this method is not convenient for the demonstration of OCT glycation by MGO, since complexes of MW different from the native enzyme are formed. Although we expected an increasing signal of the OCT band with extending time of incubation with MGO, the result is rather reverse. Nevertheless, when we compare the intensity of the bands revealed by Coomassie blue staining and both antibodies (Figure

31), we can state that the labelling of the band treated for 24 h is more intensive, considering that the present amount of the protein in this band is minimal. The clear evidence for increasing glycation of this enzyme could be brought by another immunochemical technique, e.g. competitive ELISA.

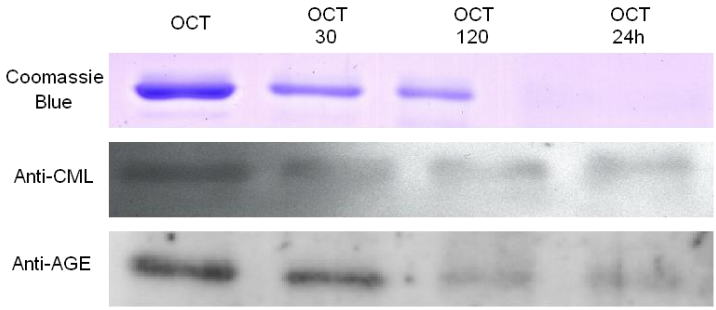

Figure 31. Comparison of the intensity of OCT bands in Coomassie blue stained gel and on the membranes treated with anti-CML antibody and anti-AGE antibody. number = time of incubation (min) with MGO

Another explanation for the failure of this method could be that both antibodies react with CML, but CEL is formed in the reaction of MGO with proteins [10]. Although the commercial anti-AGE antibody (recognising CML as a major immunological epitope) shows a cross reactivity to CEL, this reactivity can be too weak to reveal the modification in this case: the cross reactivity to CEL has been reported as 1,9 % of the reactivity to CML [51]. Another type of antibody could be tried for investigation of OCT glycation, e.g. antibody revealing modified Arg residues.

Using this method, it is not possible to localize OCT among other mitochondrial proteins, a specific antibody is needed for this purpose.

The respiration of isolated mitochondria was also measured, using a polarografic Clark electrode. The oxygen consumption of mitochondria treated with MGO for various times (0, 5, 15 min) were compared with untreated mitochondria incubated for the same time. The data is inconsistent, more experiments are needed to assess the influence of MGO on mitochondrial respiration. But interestingly, at all times of incubation, we observed a slightly lower respiratory quotient in mitochondria treated with MGO, suggesting that this compound impairs the respiratory function of mitochondria. This observation is consistent with the results from detailed studies of Rosca et al. [8, 26].

Theoretically, the loss of OCT activity *in vivo* could cause an increased ammonia level and imbalance both among amino acid and neurotransmitter levels leading to mental disturbances. The clinical importance of this phenomenon during aging should be investigated.

6 CONCLUSION

We demonstrated that methylglyoxal modifies ornithine carbamoyltransferase both *in vitro* and *ex vivo* and causes rapid and extensive decrease in its enzymatic activity. According to this study, carboxyethyllysine and cross-linked AGEs are formed. We also confirmed that MGO exerts a negative effect on mitochondrial respiration.

For further investigations, it is necessary to create anti-OCT antibody to be able to localize this enzyme among the other proteins and confirm its *in vitro* and *ex vivo* glycation by methylglyoxal. Using 2D-electrophoresis and mass spectrometry techniques, it would be interesting to localize the sites of its modification.

The loss of OCT activity during aging should be confirmed in senescent rats, to assess whether *in vitro* and *ex vivo* experiments correspond to real state. The clinical importance of this loss, especially its role in normal aging should be also investigated.

7 REFERENCES

1. **Shigenaga MK, Hagen TM, Ames BN.** Oxidative damage and mitochondrial decay in aging. *Proc Natl Acad Sci U S A.* 1994 Nov 8; 91(23): 10771-8

2. **Bakala H, Delaval E, Hamelin M, Bismuth J, Borot-Laloi C, Corman B, Friguet B.** Changes in rat liver mitochondria with aging. Lon protease-like reactivity and N(epsilon)-carboxymethyllysine accumulation in the matrix**.** *Eur J Biochem*. 2003 May; 270(10): 2295-302

3. **Ulrich P, Cerami A.** Protein glycation, diabetes, and aging. *Recent Prog Horm Res*. 2001; 56: 1-21

4. **Baynes JW.** The role of AGEs in aging: causation or correlation. *Exp Gerontol*. 2001 Sep;36(9):1527-37

5. **Voziyan PA, Khalifah RG, Thibaudeau C, Yildiz A, Jacob J, Serianni AS, Hudson BG.** Modification of proteins in vitro by physiological levels of glucose: pyridoxamine inhibits conversion of Amadori intermediate to advanced glycation end-products through binding of redox metal ions. *J Biol Chem*. 2003 Nov 21; 278(47): 46616-24

6. **Rahbar S, Figarola JL.** Inhibitors and breakers of advanced glycation endproducts (AGEs): A review. *Curr Med Chem - Imun Endoc & Metab Agents*. 2002; 2(2): 135-161

7. **Thornalley PJ.** Pharmacology of methylglyoxal: formation, modification of proteins and nucleic acids, and enzymatic detoxification - a role in pathogenesis and antiproliferative chemotherapy. *Gen Pharmacol*. 1996 Jun; 27(4): 565-73

8. **Rosca MG, Monnier VM, Szweda LI, Weiss MF.** Alterations in renal mitochondrial respiration in response to the reactive oxoaldehyde methylglyoxal. *Am J Physiol Renal Physiol*. 2002 Jul; 283(1): F52-9

9. **Speer O, Morkunaite-Haimi S, Liobikas J, Franck M, Hensbo L, Linder MD, Kinnunen PK, Wallimann T, Eriksson O.** Rapid suppression of mitochondrial permeability transition by methylglyoxal. Role of reversible arginine modification. *J Biol Chem*. 2003 Sep 12; 278(37): 34757-63

10. **Bourajjaj M, Stehouwer CD, van Hinsbergh VW, Schalkwijk CG.** Role of methylglyoxal adducts in the development of vascular complications in diabetes mellitus. *Biochem Soc Trans*. 2003 Dec; 31(Pt 6): 1400-2

11. **Chaplen FW, Fahl WE, Cameron DC.** Evidence of high levels of methylglyoxal in cultured Chinese hamster ovary cells. *Proc Natl Acad Sci U S A*. 1998 May 12; 95(10): 5533-8

12. **Suji G, Sivakami S.** Glucose, glycation and aging. *Biogerontology*. 2004;5(6): 365-73

13. **Ahmed N.** Advanced glycation endproducts--role in pathology of diabetic complications. *Diabetes Res Clin Pract*. 2005 Jan; 67(1): 3-21

14. **Biemel KM, Friedl DA, Lederer MO.** Identification and quantification of major maillard cross-links in human serum albumin and lens protein. Evidence for glucosepane as the dominant compound. *J Biol Chem*. 2002 Jul 12; 277(28): 24907-15

15. **Sell DR, Biemel KM, Reihl O, Lederer MO, Strauch CM, Monnier VM.** Glucosepane is a major protein cross-link of the senescent human extracellular matrix. Relationship with diabetes. *J Biol Chem*. 2005 Apr 1; 280(13): 12310-5

16. **Baynes JW.** Chemical modification of proteins by lipids in diabetes. *Clin Chem Lab Med*. 2003 Sep; 41(9): 1159-65

17. **Brownlee M.** Advanced protein glycosylation in diabetes and aging. *Annu Rev Med*. 1995; 46: 223-34

18. **Thornalley PJ, Battah S, Ahmed N, Karachalias N, Agalou S, Babaei-Jadidi R, Dawnay A.** Quantitative screening of advanced glycation endproducts in cellular and extracellular proteins by tandem mass spectrometry. *Biochem J*. 2003 Nov 1; 375(Pt 3): 581-92

19. **Vlassara H, Palace MR.** Glycoxidation: the menace of diabetes and aging. *Mt Sinai J Med*. 2003 Sep; 70(4): 232-41

20. **Giardino I, Edelstein D, Brownlee M.** BCL-2 expression or antioxidants prevent hyperglycemia-induced formation of intracellular advanced glycation endproducts in bovine endothelial cells. *J Clin Invest.* 1996 Mar 15; 97(6): 1422-8

21. **Seidler, N.** Carbonyl-Induced Enzyme Inhibition: Mechanisms and New Perspectives. *Current Enzyme Inhibition*. 2005; 1: 21-27

22. **Poggioli S, Bakala H, Friguet B.** Age-related increase of protein glycation in peripheral blood lymphocytes is restricted to preferential target proteins. *Exp Gerontol*. 2002 Oct-Nov; 37(10-11): 1207-15

23. **Giardino I, Edelstein D, Brownlee M.** Nonenzymatic glycosylation in vitro and in bovine endothelial cells alters basic fibroblast growth factor activity. A model for intracellular glycosylation in diabetes. *J Clin Invest*. 1994 Jul; 94(1): 110-7

24. **Padival AK, Crabb JW, Nagaraj RH.** Methylglyoxal modifies heat shock protein 27 in glomerular mesangial cells. *FEBS Lett*. 2003 Sep 11; 551(1-3): 113-8

25. **Zahner D, Liemans V, Malaisse-Lagae F, Malaisse WJ.** Non-enzymatic glycation of phosphoglucoisomerase. *Diabetes Res*. 1989 Dec; 12(4): 165-8

26. **Rosca MG, Mustata TG, Kinter MT, Ozdemir AM, Kern TS, Szweda LI, Brownlee M, Monnier VM, Weiss MF.** Glycation of mitochondrial proteins from diabetic rat kidney is associated with excess superoxide formation. *Am J Physiol Renal Physiol*. 2005 Aug; 289(2): F420-30

27. **Vostry M**. *Glycoxidative changes of mitochondrial enzymes*. Plzeň, 2005. Diploma thesis, Charles university in Prague, Faculty of pharmacy in Hradec Králové, Department of biochemical sciences

28. **Shi D, Morizono H, Yu X, Tong L, Allewell NM, Tuchman M.** Human ornithine transcarbamylase: crystallographic insights into substrate recognition and conformational changes. *Biochem J.* 2001 Mar 15; 354(Pt 3): 501-9

29. **Legrain C, Villeret V, Roovers M, Tricot C, Clantin B, Van Beeumen J, Stalon V, Glansdorff N.** Ornithine carbamoyltransferase from Pyrococcus furiosus. *Methods Enzymol*. 2001; 331: 227-35

30. **Shi D, Morizono H, Aoyagi M, Tuchman M, Allewell NM.** Crystal structure of human ornithine transcarbamylase complexed with carbamoyl phosphate and L-norvaline at 1.9 A resolution. *Proteins*. 2000 Jun 1; 39(4): 271-7

31. **Marshall M, Cohen PP.** Ornithine transcarbamylase from Streptococcus faecalis and bovine liver. I. Isolation and subunit structure. *J Biol Chem*. 1972 Mar 25; 247(6): 1641-53

32. **Shi D, Morizono H, Ha Y, Aoyagi M, Tuchman M, Allewell NM.** 1.85-A resolution crystal structure of human ornithine transcarbamoylase complexed with

N-phosphonacetyl-L-ornithine. Catalytic mechanism and correlation with inherited deficiency. *J Biol Chem*. 1998 Dec 18; 273(51): 34247-54

33. <http://www.expasy.org/sprot/>

34. <http://npsa-pbil.ibcp.fr/cgi-bin/npsa_automat.pl?page=npsa_clustalw.html>

35. **Labedan B, Boyen A, Baetens M, Charlier D, Chen P, Cunin R, Durbeco V, Glansdorff N, Herve G, Legrain C, Liang Z, Purcarea C, Roovers M, Sanchez R, Toong TL, Van de Casteele M, van Vliet F, Xu Y, Zhang YF.** The evolutionary history of carbamoyltransferases: A complex set of paralogous genes was already present in the last universal common ancestor. *J Mol Evol*. 1999 Oct; 49(4): 461-73

36. **Hartshorn MJ.** AstexViewer: a visualisation aid for structure-based drug design. *J Comput Aided Mol Des*. 2002 Dec; 16(12): 871-81

37. <http://swissmodel.expasy.org/repository/>

38. **Naumoff DG, Xu Y, Glansdorff N, Labedan B.** Retrieving sequences of enzymes experimentally characterized but erroneously annotated: the case of the putrescine carbamoyltransferase. *BMC Genomics*. 2004 Aug 2; 5(1): 52

39. **Paschen SA, Neupert W.** Protein import into mitochondria. *IUBMB Life*. 2001 Sep-Nov; 52(3-5): 101-12

40. **Gordon N.** Ornithine transcarbamylase deficiency: a urea cycle defect. *Eur J Paediatr Neurol*. 2003; 7(3): 115-21

41. **Brosnan JT.** Glutamate, at the interface between amino acid and carbohydrate metabolism. *J Nutr*. 2000 Apr; 130(4S Suppl): 988S-90S

42. **Shambaugh GE 3rd.** Urea biosynthesis I. The urea cycle and relationships to the citric acid cycle. *Am J Clin Nutr*. 1977 Dec; 30(12): 2083-7

43. **Voet D, Voetová JG.** *Biochemie*. Praha: Victoria publishing, 1995. ISBN 80-85605-44-9

44. <http://138.192.68.68/bio/Courses/biochem2/AminoAcids/UreaCycle.html>

45. **Watford M.** Glutamine and glutamate metabolism across the liver sinusoid. *J Nutr*. 2000 Apr; 130 (4S Suppl): 983S-7S

46. **Watford M.** Hepatic glutaminase expression: relationship to kidney-type glutaminase and to the urea cycle. *FASEB J*. 1993 Dec; 7(15): 1468-74

47. **Wu G.** Intestinal mucosal amino acid catabolism. *J Nutr*. 1998 Aug; 128(8): 1249-52

48. **Wu G, Morris SM Jr**. Arginine metabolism: nitric oxide and beyond. *Biochem J*. 1998 Nov 15; 336 (Pt 1): 1-17

49. **Tuchman M, Morizono H, Rajagopal BS, Plante RJ, Allewell NM.** The biochemical and molecular spectrum of ornithine transcarbamylase deficiency. *J Inherit Metab Dis*. 1998; 21 Suppl 1: 40-58

50. **Verbeke P, Perichon M, Borot-Laloi C, Schaeverbeke J, Bakala H.** Accumulation of advanced glycation endproducts in the rat nephron: link with circulating AGEs during aging. *J Histochem Cytochem*. 1997 Aug; 45(8): 1059-68

51. **Ikeda K, Higashi T, Sano H, Jinnouchi Y, Yoshida M, Araki T, Ueda S, Horiuchi S.** N (epsilon)-(carboxymethyl)lysine protein adduct is a major immunological epitope in proteins modified with advanced glycation end products of the Maillard reaction. *Biochemistry*. 1996 Jun 18; 35(24): 8075-83

LIST OF ABBREVIATIONS

2D-PAGE	Two dimension polyacrylamide gel electrophoresis
3-DG	3-Deoxyglucosone
Aa	Amino acids
ADP	Adenosine diphosphate
AGE	Advanced glycation end-product
ALE	Advanced lipoxidation end-product
ALI	Arginine-lysine imidazole
AMP	Adenosine monophosphate
APS	Ammonium persulphate
ATP	Adenosine triphosphate
AWB	Amersham ECL Advance Western Blotting Detection Kit (GE Healthcare)
BSA	Bovine serum albumin
CEL	N^{ε} Carboxyethyllysine
CMA	Carboxymethylarginine
CML	N^{ε} Carboxymethyllysine
CML-BSA	Carboxymethylated bovine serum albumin
CP	Carbamoyl phosphate
Da	Dalton
EC	Enzyme commission
EDTA	Ethylene diamine tetraacetic acid
GDH	Glutamate dehydrogenase
GO	Glyoxal
GODIC	Glyoxal-derived imidazoline cross-link
GOLD	Glyoxal-derived lysine dimmer
kDa	Kilodalton
LBBCV	Laboratoire de Biologie et Biochimie Cellulaire du Vieillissement
LDL	Low-density lipoproteid
MGO	Methylglyoxal
MODIC	Methylglyoxal-derived imidazoline cross-link
MOLD	Methylglyoxal-derived lysine dimmer

MS/MS	Tandem mass spectrometry
MW	Molecular weight
NADH	Nicotinamide adenine dinucleotide (reduced form)
OCT	Ornithine carbamoyltransferase
OCTD	Ornithine carbamoyltransferase deficiency
ORN	Ornithine
OTC	Ornithine transcarbamylase
PALO	N-phosphonacetyl-L-ornithine
PTCase	Putrescine transcarbamylase
PVFD	Polyvinylidene difluoride
Rf	Retention factor
ROS	Reactive oxygen species
SD	Standard deviation
S. faecalis	*Streptococcus faecalis*
SDS	Sodium dodecyl sulphate
SDS-PAGE	Sodium dodecyl sulphate polyacrylamide gel electrophoresis
Std	Standard
TCA	Trichloracetic acid
TCA cycle	Tricarboxylic acid cycle
TEMED	N,N,N',N'- tetramethyl ethylene diamine
Tris	Tris(hydroxymethyl)aminomethane
U	Unit
WB	Western blotting (analysis)
WP	SuperSignal West Pico Chemiluminiscent Substrate (Pierce)
β-ME	β-mercaptoethanol